

# Bose-Einstein Interference in the Passage of a Jet in a Dense Medium<sup>†</sup>

Cheuk-Yin Wong

*Physics Division, Oak Ridge National Laboratory, Oak Ridge, TN 37831*

(Dated: November 9, 2018)

When a jet collides coherently with many parton scatterers at very high energies, the Bose-Einstein symmetry with respect to the interchange of the virtual bosons leads to a destructive interference of the Feynman amplitudes in most regions of the momentum transfer phase space but a constructive interference in some other regions of the momentum transfer phase space. As a consequence, the recoiling scatterers have a tendency to come out collectively along the incident jet direction, each carrying a substantial fraction of the incident jet longitudinal momentum. The manifestation of the Bose-Einstein interference as collective recoils of the scatterers along the jet direction may have been observed in angular correlations of hadrons associated with a high- $p_T$  trigger in high-energy heavy-nuclei collisions at RHIC and LHC.

PACS numbers: 25.75.-q 25.75.Dw

## I. INTRODUCTION

Recently at RHIC and LHC, angular correlations of produced hadron pairs in AuAu, PbPb, and  $pp$  collisions have been measured to obtain the yield of produced pairs as a function of  $\Delta\phi$  and  $\Delta\eta$ , where  $\Delta\phi$  and  $\Delta\eta$  are the azimuthal angle and pseudorapidity differences of the produced pair. The correlations appear in the form of a “ridge” that is narrow in  $\Delta\phi$  at  $\Delta\phi \sim 0$  and  $\Delta\phi \sim \pi$ , but relatively flat in  $\Delta\eta$ . They have been observed in high-energy AuAu collisions at RHIC by the STAR Collaboration [1–19], the PHENIX Collaboration [20–24], and the PHOBOS Collaboration [25], with or without a high- $p_T$  trigger [2, 14–18]. They have also been observed in  $pp$  and PbPb collisions at the LHC by the CMS Collaboration [26–28], the ATLAS Collaboration [29], and the ALICE Collaboration [30].

Subsequent to the observation of the  $\Delta\phi$ - $\Delta\eta$  angular correlations, a momentum kick model [31–39] was put forth to explain the “ridge” phenomenon, along with many other models [40–74]. The model identifies ridge particles as medium partons, because of the centrality dependence of the ridge particle yield and the similarity between the temperature and baryon/meson ratio of ridge particles with those of the bulk medium. The model assumes that these medium partons have an initial rapidity plateau distribution, and when they suffer a collision with a jet produced in the collision, they receive a momentum kick along the jet direction, which will be designated as the longitudinal direction. The physical contents of the momentum kick model lead to features consistent with experimental observations: (i) the longitudinal momentum kicks from the jet to the medium partons along the jet direction give rise to the  $\Delta\phi \sim 0$  correlations on the near-side [1, 3, 31–35], (ii) the medium

parton initial rapidity plateau distribution shows up as a ridge along the  $\Delta\eta$  direction [1, 3, 31–35, 37, 38], (iii) the displaced parton momentum distribution of the kicked medium partons leads to a peak at  $p_T \sim 1$  GeV/c in the  $p_T$  distribution of the kicked partons [18, 33, 38], and (iv) the kicked medium partons therefore possess a correlation of  $|p_{1T}| \sim |p_{2T}| \sim 1$  GeV, without a high- $p_T$  trigger, for both the near side and the away side [18, 38]. The model has been successful in describing extensive sets of triggered associated particle data of the STAR Collaboration, the PHENIX Collaboration, and the PHOBOS Collaboration, over large regions of  $p_t$ ,  $\Delta\phi$ , and  $\Delta\eta$ , in many different phase space cuts and  $p_T$  combinations, including dependencies on centralities, dependencies on nucleus sizes, and dependencies on collision energies [31–38].

The phenomenological success of the momentum kick model raises relevant questions about the theoretical foundations for its basic assumptions. While the rapidity plateau structure of the medium parton distribution may have its origin in the Wigner function of particles produced in the fragmentation of a string (or flux tube) [36], or in a color-glass condensate [47], the origin of the postulated longitudinal momentum kick along the jet direction in the model poses an interesting puzzle. If each of the jet-(medium parton) collision were a two-body elastic collision, it would lead only to a dominantly forward scattering and a small longitudinal momentum transfer to the medium scatterers along the jet direction. The hard longitudinal momentum kick (of order GeV) received by the medium scatterers along the jet direction in the momentum kick model is unlikely to originate from incoherent two-body collisions.

From an observational viewpoint, the experimental observation that many medium partons come out along the jet longitudinal direction with  $\Delta\phi \sim 0$  implies the presence of collective recoils of the medium partons, each of which must have acquired a substantial longitudinal momentum transfer (momentum kick) along the jet direction from the jet. What is the origin of such collective recoils, in the interaction of the jet with medium partons?

<sup>†</sup>Based in part on a talk presented at the Fourteenth Meeting of the Chinese Nuclear Physical Society in Intermediate and High Energy Nuclear Physics, Qufu, Shandong, China, October 20–24, 2011.

As the high- $p_T$  trigger particles under experimental consideration have a momentum of order a few GeV [1–3, 20–23, 27–30], we therefore consider incident jets with an initial momentum of order 10 GeV. Strictly speaking, jets with an initial momentum of order 10 GeV should be more appropriately called “mini-jets” [75]. For brevity of nomenclature, we continue to use the term “jet” to represent mini-jets.

In the collision of a jet  $p=(p_0, \mathbf{p})$  with  $n$  medium partons, how dense must the medium be for the multiple collisions to become a single coherent  $(1+n)$ -body collision, instead of a sequence of  $n$  incoherent 2-body collisions? It is instructive to find out the conditions on the medium density and the energy of the incident jet that determine whether the set of multiple collisions are coherent or incoherent. For such a purpose, we consider a binary collision between the incident fast particle  $p$  and a medium scatterer  $a_i$  with the exchange of a boson, in the medium center-of-momentum frame. The longitudinal momentum transfer  $q_z$  for the binary collision can be obtained from the transverse momentum transfer  $q_T$  by  $q_z \sim q_T^2/2p_0$ . The longitudinal momentum transfer is associated with a longitudinal coherence length  $\Delta z_{\text{coh}} \sim \hbar/q_z \sim 2\hbar p_0/q_T^2$  that specifies the uncertainties in the longitudinal locations at which the virtual boson is exchanged between the fast particle and the scatterer. The time it takes for the fast particle to travel the distance of the longitudinal coherence length,  $2p_0\hbar/q_T^2 c$ , can also be called the virtual boson formation time.

The nature of the multiple scattering process can be inferred by comparing the longitudinal coherence length  $\Delta z_{\text{coh}}$  with the mean free path  $\lambda$  of the jet in the dense medium that depends not only on the density of the medium but also on the binary collision cross section.

If  $\Delta z_{\text{coh}} \ll \lambda$ , then a single binary collision is well completed before another binary collision begins, and the multiple collision process consists of a sequence of  $n$  incoherent two-body collisions. On the other extreme, if

$$\Delta z_{\text{coh}} \sim 2\hbar p_0/q_T^2 \gg \lambda, \quad (1)$$

then a single binary collision is not completed before another one begins, and the multiple collision process consists of a set of coherent collisions as a single  $(1+n)$ -body collision. For a set of initial and final states in such a coherent  $(1+n)$ -body collision, there are  $n!$  different trajectories in the sequence of collisions along  $\Delta z_{\text{coh}}$  at which various virtual bosons are exchanged. By Bose-Einstein symmetry, the total Feynman amplitude is then the sum of the  $n!$  amplitudes for all possible interchanges of the exchanged virtual bosons. The summation of these  $n!$  Feynman amplitudes and the accompanying interference constitute the Bose-Einstein interference in the passage of the fast particle in the dense medium.

In high energy central collisions between heavy nuclei such as those at RHIC and LHC, both jets and dense medium are produced after each collision. The jets will collide with partons in the dense medium, and these collisions may satisfy the condition for coherent collisions.

In a binary collision at RHIC and LHC, the longitudinal coherent length  $\Delta z_{\text{coh}}$  is of order 25 fm, for a typical transverse momentum transfer of  $q_T \sim 0.4$  GeV/c from a jet of momentum  $p_0 \sim 10$  GeV/c to a medium parton. The longitudinal coherent length  $\Delta z_{\text{coh}}$  is much greater than the radius  $R$  of a large nucleus. On the other hand, the away side jet is quenched by the dense medium in the most central AuAu collisions at RHIC and LHC [76–82], and the near-side jet collides with about 4-6 medium partons [31]–[38]. Therefore, one can infer that the mean-free path  $\lambda$  for the collision of the jet with medium partons is much smaller than the nuclear radius  $R$ . In high-energy central nuclear collisions at RHIC and LHC, the collision of a fast jet with medium scatterers satisfy the following condition

$$\Delta z_{\text{coh}} \sim 2\hbar p_0/q_T^2 \gg R \gg \lambda. \quad (2)$$

As a consequence, the multiple collision process constitutes a set of coherent collisions. There will be Bose-Einstein interference effects in the passage of the jet in the dense medium.

In this connection of Bose-Einstein interference, we note that Bose-Einstein interference effects in high-energy QED and QCD collisions have been observed previously by many workers [83–90]. In the emission or absorption of  $n$  identical bosons from an energetic fermion in Abelian and non-Abelian gauge theories leading to an on-mass-shell final fermion, the Bose-Einstein symmetry with respect to the interchange of virtual bosons leads to the sum of a the set of  $n!$  Feynman amplitudes that turns out simply to be a product of delta functions. These distributions may be thought of as peaked interference patterns produced by the coherent addition of various symmetrized broad Feynman amplitudes [90]. In the collision of two fermions, the sum of the ladder and cross-ladder diagrams also exhibits remarkable Bose-Einstein interference leading to similar products of delta functions and the eikonal approximation [83–90].

We would like to study similar interference effects for the case of the multiple collisions of a jet parton with many parton scatterers. We wish to explore whether such a Bose-Einstein interference may be the origin of the longitudinal momentum kick. As the interference arises from the coherent collision of more than one particle, it is clearly a many-body effect that occurs with two or more scatterers.

The interference of Feynman amplitudes is only one of the effects of coherent collisions. There is another important effect that accompanies the coherent  $(1+n)$ -body collision and changes the nature of the collision process. It shows up as an increase in the number of degrees of freedom. In a sequence of  $n$  incoherent two-body collisions or quasi-elastic collisions, there are two degrees of freedom in each two-body collision, which can be chosen to be  $\mathbf{q}_{iT} = (q_{iT}, \phi_i)$ . The sequence of  $n$  incoherent or quasi-elastic two-body collisions contains only  $2n$  transverse momentum transfer degrees of freedom,  $\{\mathbf{q}_{1T}, \mathbf{q}_{2T}, \mathbf{q}_{3T}, \dots, \mathbf{q}_{nT}\}$ . The longitudinal momen-

tum transfer  $q_{iz}$  in each individual jet-parton collision is a dependent variable, depending on the corresponding transverse momentum transfer as  $q_{iz} \sim |\mathbf{q}_{iT}|^2/2p_0$ . In contrast, in the case of coherent collisions of the jet with  $n$  particles, there are  $3n - 1$  degrees of freedom, after the  $3(n + 1)$  degrees of freedom are reduced by the constraints of the conservation of energy and momentum. The degrees of freedom increases from  $2n$  for incoherent collision and quasi-elastic collisions to  $3n - 1$  for coherent collisions. We can choose the  $3n - 1$  independent variables to be  $\{\mathbf{q}_{1T}q_{1z}, \mathbf{q}_{2T}q_{2z}, \mathbf{q}_{3T}q_{3z}, \dots, \mathbf{q}_{nT}q_{nz}\}$  for coherent collisions, subject to a single condition of an overall energy conservation. Thus in the case of coherent collisions, the set of longitudinal momentum transfers,  $\{q_{iz}, i = 1, 2, \dots, n\}$ , can also be independent variables with their own probability distribution functions, depending on the sum of  $n!$  symmetrized Feynman amplitudes. The recoiling scatterers share the longitudinal momentum of the incident jet. The  $q_{iz}$  degrees of freedom allow the medium partons to acquire substantial fractions of the longitudinal momentum of the incident jet, as we shall demonstrate in Section V of this paper.

In the problem of the passage of a jet in a dense medium, the multiple collision process of the jet with medium partons is usually examined in the potential model [77–81, 91–93], as in the Glauber theory [94]. It should be noted that the occurrence of coherent collision discussed here coincide with the condition for multiple scattering in the Glauber theory given by Eq. (173) of [94] as

$$p_0 a^2 / \hbar \gg R, \quad (3)$$

where  $R$  is the dimension of the medium, and  $a$  is the range of the interaction which can be related to the average transverse momentum transfer by  $a \sim \hbar/q_T$ . Thus the Glauber's condition for multiple scattering is

$$\hbar p_z / q_T^2 \gg R. \quad (4)$$

As the dimension of the medium is presumably much greater than the mean free path  $\lambda$  between collisions, condition (3) for Glauber's multiple scattering is consistent with

$$\hbar p_z / q_T^2 \gg R \gg \lambda \quad (5)$$

that is nearly the same as the coherent condition (2) we discussed here, except for an unimportant difference of a factor of two.

The near-coincidence of the conditions for coherent collisions of Eqs. (2) and (5) indicates that the totality of coherent collisions can be further divided according to the degree of incident jet longitudinal momentum losses. There are elastic and quasi-elastic coherent collisions with nearly no scatterer recoils and little loss of the incident jet longitudinal momentum that are at the center of Glauber-type potential model theories. There are also coherent collisions in which scatterers can undergo longitudinal recoils and the incident jet can lose a

substantial longitudinal momentum arising from the recoils of scatterers. The elastic and quasi-elastic coherent collision processes can be adequately studied in the potential model [77–81, 91–94], with the assumption that the scatterers suffer approximately no recoils and appear in the form of potential centers around which the projectile traverses.

We wish to investigate coherent collisions in the entire domain of longitudinal scatterers recoils and the corresponding incident jet longitudinal momentum loss due to these recoils. For a general treatment of longitudinal recoils of scatterers, the Glauber-type potential model cannot really be used. It is inadequate because it is restricted to elastic and quasi-elastic collisions and does not allow the scatterer longitudinal recoils to be independent degrees of freedom. For well-founded reasons which we shall discuss in detail in Section II, we shall forgo the potential model but turn to the Feynman amplitude approach to study the longitudinal recoils of the scatterers in a general treatment of coherent collisions.

In the remaining parts of the manuscript, we shall consider implicitly only coherent multiple collisions of the jet with medium partons unless indicated otherwise. In Section III, we examine (coherent) multiple collisions of an energetic fermion with fermion scatterers in the Abelian gauge theory to discuss how the Bose-Einstein symmetry in the Feynman amplitudes can lead to a destructive interference over most regions of phase space but a constructive interference in some other regions of phase space. In Section IV, we study the cross section for such a multiple collision process. In Section V, we examine the consequences of the constraints on the recoils of the scatterers and find that the scatterers tend to come out collectively along the incident jet direction, each scatterer acquiring approximately  $1/2n$  fraction of the longitudinal momentum of the incident jet. In Section VI, we examine the case for the coherent collision of an energetic fermion with fermion scatterers in the non-Abelian gauge theory. In Section VII, we generalize our considerations to the collision of a gluon jet on quark scatterers. In Section VIII, we examine the collision of a gluon or a fermion jet on gluon scatterers. In Section IX, we study the longitudinal momentum distribution for gluon scatterers and distinguish it from the longitudinal momentum distribution for quark scatterers. In Section X, we examine the signatures of the Bose-Einstein interference in the passage of a jet in a medium and compare these signatures with experimental data. In Section XI, we present our conclusions and discussions.

## II. THE POTENTIAL MODEL VERSUS THE FEYNMAN AMPLITUDE APPROACH

The potential model of multiple collisions [77–81, 91–94] has been a useful tool to study the energy loss of a jet as it passes through a dense medium in elastic and quasi-elastic scatterings. It can also be adequately used

to study the longitudinal momentum transfers  $q_{iz}$  from the jet to the scatterers in these elastic and quasi-elastic processes. The potential model gives the longitudinal recoil momentum

$$q_{iz} \sim |\mathbf{q}_{iT}|^2/2p_0, \quad (6)$$

for each jet-scatterer collision, in either coherent or incoherent collisions.

We shall see that in the Feynman amplitude approach the probability distribution for the longitudinal recoil  $q_{iz}$  includes not only the probability for quasi-elastic processes with little scatterers longitudinal recoils but also a significant probability for the scatterers to recoil with a substantial fraction of the incident jet longitudinal momentum. It is therefore important to inquire which of the two different approaches should be used to investigate the longitudinal recoils of the scatterers in a general treatment of coherent collisions that are at the focus of our attention.

It is instructive to review how the longitudinal recoils of the scatterers are determined in the two different approaches. In the potential model [77–81, 91–94], the medium parton scatterers are assumed to be fixed in space and the scatterings between the incident particle and the medium scatterers are represented by potentials with the positions of the scatterers as static centers, as in the Glauber model for potential scattering [94]. By using *static* scatterer centers, the range of applicability of the potential model is limited to elastic or quasi-elastic scatterings with small momentum transfer  $\mathbf{q}_i$ . Furthermore, we can trace how  $\mathbf{q}_i = (\mathbf{q}_{iT}, q_{iz})$  is determined in the potential model, in the collision of the jet with the  $i$ th scatterer. After passing through the potential generated by the  $i$ th scatterer, the trajectory of the incident jet is obtained and the transverse momentum transfer  $\mathbf{q}_{iT}$  determined. The longitudinal momentum transfer  $q_{iz}$  from the jet to the scatterer is subsequently calculated to ensure longitudinal momentum conservation. Hence the longitudinal momentum transfer from the jet to the  $i$ th scatterer is determined as  $q_{iz} \sim \mathbf{q}_{iT}^2/2p_0$ , as given in Eq. (6). As the longitudinal momentum transfer  $q_{iz}$  is determined completely by  $\mathbf{q}_{iT}$  and  $p_0$ , it is no longer an independent dynamical variable. It is in effect a frozen and dependent quantity. Not only is the potential model limited to scattering with small momentum transfers  $\mathbf{q}_i$ , the model is also limited to cases in which the longitudinal momentum transfers  $q_{iz}$  from the jet to the scatterers are no longer independent dynamical variables.

In the potential model with many scatterers, the total potential is the sum of all scatterer potentials. In the coherent collisions limit, the wave function of the incident jet becomes [94]

$$\psi(z) = \exp\{ik(z - z_0) + i\chi_{\text{tot}}(b, z)\}, \quad (7)$$

where the phase  $\chi_{\text{tot}}(b, z)$  is the sum of the scattering

phases from scatterer potentials  $V_i$  centered at  $\{\mathbf{b}_i, z_i\}$ ,

$$\chi_{\text{tot}}(b, z) = -\frac{i}{\hbar v} \int_{z_0}^z dz' \sum_{i=1}^n V_i(\mathbf{b} - \mathbf{b}_i, z' - z_i). \quad (8)$$

The width of the transverse momentum distribution of the incident jet is broadened by collisions with scatterers. From the broadening of the transverse momentum distribution associated with the transverse momentum transfer  $\mathbf{q}_{iT}$  due to the interaction of the jet with the  $i$ th scatterer, one infers that the corresponding longitudinal momentum transfer to the  $i$ th scatterer is given again by  $q_{iz} \sim |\mathbf{q}_{iT}|^2/2p_0$  as in Eq. (6) in the coherent collision limit.

From the above review, we recognize that in the potential model, all recoils of the scatterers have been assumed to be zero initially to allow a static description of the centers of the scatterers. The scatterer longitudinal recoils are only subsequently corrected as an appendage to the dynamics of the transverse deflection of the incident jet. Such a potential model may be adequate for incoherent collisions and for quasi-elastic coherent collisions in which the longitudinal momentum transfers to the scatterers are very small.

As the longitudinal recoils of the scatterers are at the focus of our attention, it is important to realize that the potential model cannot be used to examine the longitudinal recoils of the scatterers in a general treatment where one wants to explore the behavior of the probability distribution for the scatterer longitudinal momentum transfer over a large domain, or in regions where there may be a high probability for recoiling scatterers to share substantial fractions of the longitudinal momentum of the incident jet. A general treatment of coherent collisions necessitates the use of the longitudinal recoils of the scatterers as independent dynamical variables. The longitudinal recoils of the scatterers are however not allowed to be independent dynamical variables in the potential model. This leads us to forgo the potential model and to turn to the use of Feynman amplitudes for coherent collisions.

In the Feynman amplitude approach such as given in what follows for a set of the initial momenta of the jet and scatterers, the  $(n+1)$  final momenta involved in the collision process are dynamical variables. The Feynman amplitudes give the probability amplitudes for various reaction channels as a function of these dynamical variables. In particular, the longitudinal momenta of the recoiling scatterers and the corresponding longitudinal momentum transfers from the jet to the scatterers are dynamical variables, in contrast to the potential model in which they are frozen and dependent quantities. Feynman amplitudes with explicit scatterer momenta on the external legs are the proper tools to examine the probability amplitudes as a function of the longitudinal recoils of the scatterers.

In the Feynman amplitude approach, the momenta of recoiling scatterers are intimately linked together with



the momentum of the incident jet in various Feynman amplitudes and their corresponding symmetrized  $n!$  permutations. The  $n$  scatterers and the jet comprise an  $(n+1)$ -body system, with  $3(n+1)$  degrees of freedom constrained by the four-dimensional energy and momentum conservation. Among the  $3(n+1)$  degrees of freedom are the transverse and longitudinal momentum transfers from the jet to the scatterers,  $(\mathbf{q}_{iT}, q_{iz})$ ,  $i = 1, \dots, n$ . As the recoiling scatterers and the recoiling jet are tied together by the coherent collision, they can share the initial longitudinal momentum of the jet. We shall find from the Feynman amplitude approach that  $\langle q_{iz} \rangle$  can be a substantial fraction of the longitudinal momentum of the incident jet (see Section IV). The potential model in contrast gives the result  $q_{iz} = |\mathbf{q}_{iT}|^2/2p_0$  that cannot be relied upon for a general coherent collision, because (i) the potential model confines the system to regions of small  $q_{iz}$ , (ii) as it has been designed for elastic and quasi-elastic processes, the potential model does not allow  $q_{iz}$  to be independent dynamical variables, and (iii) as a consequence, the potential model precludes the exploration into other  $q_{iz}$  regions where the probability distribution as a function of  $q_{iz}$  may be large in coherent collisions.

In the general treatment of coherent collisions with the jet, we are therefore justified to forgo the potential model and use the Feynman amplitude approach to study the transverse and longitudinal recoils of parton scatterers.

### III. BOSE-EINSTEIN INTERFERENCE OF THE FEYNMAN AMPLITUDES

We consider a jet  $p$  passing through a dense medium and making (coherent) multiple collisions with medium partons. The assembly of medium partons has an initial momentum distribution. We choose to work in the center-of-momentum frame of the parton scatterers  $\{a_1, a_2, \dots, a_n\}$ . We select the longitudinal  $z$ -axis to be along the momentum of the incident jet.

As an illustration of the salient features of the interference of the Feynman amplitudes, we consider first multiple collisions of a fermion  $p$  with rest mass  $m$  and two fermion scatterers  $a_1$  and  $a_2$  with rest masses  $m_1$  and  $m_2$  in  $p + a_1 + a_2 \rightarrow p' + a'_1 + a'_2$ . We study this problem in the Abelian gauge theory in this section and in the non-Abelian gauge theory in Section VI. We shall consider the collision of gluons in Section VII.

Using the Feynman rules as in Ref. [84], the Feynman amplitude for diagram 1(a) is given by [95, 96]

$$M_a = -g^4 \bar{u}(\mathbf{p}') \gamma_\nu \frac{1}{\not{p} - \not{q}_1 - m + i\epsilon'} \gamma_\mu u(\mathbf{p}) \times \frac{1}{q_2^2} \bar{u}(\mathbf{a}_2') \gamma_\nu u(\mathbf{a}_2) \frac{1}{q_1^2} \bar{u}(\mathbf{a}_1') \gamma_\mu u(\mathbf{a}_1). \quad (9)$$

If the spatial separation between the scatterers is so large such that  $\lambda \gg \Delta z_{\text{coh}}$  the fast particle is nearly on the mass shell after the first collision and the diagram

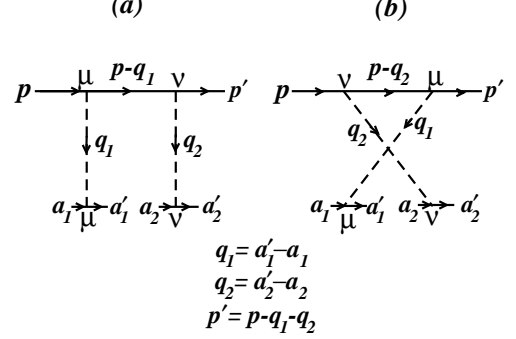


FIG. 1: Feynman diagrams for the collision of a fast fermion  $p$  with medium fermions  $a_1, a_2$ , with the emission and absorption of virtual bosons of momenta  $q_1$  and  $q_2$ .

1(a) suffices. It can be cut into two disjoint pieces. The collision process consists effectively of a sequence of two two-body collisions. We shall show in Section IV that for a ladder diagram of the type shown in Fig. 1(a) for quasi-elastic collision, with intermediate fast particles assumed to be on the mass shell and  $q_{i0} \sim 0$ , the  $(1+n)$  body cross section is a product of  $n$  two-body cross sections.

On the other hand, if the collision is characterized by  $\lambda \ll \Delta z_{\text{coh}}$  the collision process is in a coherent  $(1+2)$ -body collision. There is an additional Feynman amplitude  $M_b$  for diagram 1(b), obtained by making a symmetrized permutation of the bosons in diagram 1(a),

$$M_b = -g^4 \bar{u}(\mathbf{p}') \gamma_\mu \frac{1}{\not{p} - \not{q}_2 - m + i\epsilon'} \gamma_\nu u(\mathbf{p}) \times \frac{1}{q_2^2} \bar{u}(\mathbf{a}_2') \gamma_\nu u(\mathbf{a}_2) \frac{1}{q_1^2} \bar{u}(\mathbf{a}_1') \gamma_\mu u(\mathbf{a}_1). \quad (10)$$

The trajectories for diagram 1(a) and 1(b) are both possible paths in a coherent collision, leading from a set of initial states to a set of final states. By Bose-Einstein symmetry, the total amplitude  $M$  for coherent collisions is the symmetrized sum of  $M_a$  and  $M_b$ .

We consider the high-energy limit and assume the conservation of helicity with

$$\{p_0, |\mathbf{p}|, p'_0, |\mathbf{p}'|\} \gg \{|\mathbf{a}_i|, q_0, |\mathbf{q}_i|\} \gg m, \text{ for } i = 1, 2.$$

We shall later find that  $\langle q_{iz} \rangle/p_z$  is of order  $1/2n$ . The above high-energy limit of  $\{p_0, |\mathbf{p}|, p'_0, |\mathbf{p}'|\} \gg \{q_0, |\mathbf{q}_i|\}$  provides a reasonable approximation to the gross features of the collision processes. Higher order corrections to this approximation will lead to refinements that will be the subjects of future investigations.

In this high-energy limit, we have approximately [84]

$$\bar{u}(\mathbf{a}') \gamma_\mu u(\mathbf{a}) \sim \sqrt{\frac{a_0 + m}{a'_0 + m}} \frac{a'_\mu}{2m} + \sqrt{\frac{a'_0 + m}{a_0 + m}} \frac{a_\mu}{2m} \equiv \frac{\tilde{a}_\mu}{m} \quad (11)$$

$$\frac{1}{\not{p} - \not{q}_1 - m + i\epsilon'} \gamma_\nu u(p) \sim -\frac{\not{p} - \not{q}_1 + m}{2p \cdot q_1 - i\epsilon} \gamma_\nu u(p), \quad (12)$$

$$\bar{u}(p) \gamma_\nu (\not{p} - \not{q}_1 + m) \gamma_\mu u(p) \sim \frac{2p_\nu p_\mu}{m}, \quad (13)$$

where  $\epsilon$  is a small positive quantity. We shall be interested in the case in which the fermion  $p'$  after the collision is outside the medium and is on the mass shell. The mass shell condition can be expressed as

$$(p - q_1 - q_2)^2 - m^2 \sim -2p \cdot q_1 - 2p \cdot q_2 \sim 0. \quad (14)$$

The symmetrized sum of the Feynman amplitudes  $M_a$  and  $M_b$  in the high-energy limit is

$$M \sim \frac{g^4}{2m} \frac{2p \cdot \tilde{a}_1}{m_1 q_1^2} \frac{2p \cdot \tilde{a}_2}{m_2 q_2^2} \left( \frac{1}{2p \cdot q_1 - i\epsilon} + \frac{1}{2p \cdot q_2 - i\epsilon} \right). \quad (15)$$

Note that the amplitudes  $M_a$  and  $M_b$  correlate with each other because of the mass-shell condition (14). The real parts of the amplitudes destructively cancel, and the imaginary parts interfere and add constructively, to result in sharp distributions at  $p \cdot q_1 \sim 0$  and  $p \cdot q_2 \sim 0$ ,

$$M \sim \frac{g^4}{2m} \frac{2p \cdot \tilde{a}_1}{m_1 q_1^2} \frac{2p \cdot \tilde{a}_2}{m_2 q_2^2} \left\{ i\pi \Delta(2p \cdot q_1) + i\pi \Delta(2p \cdot q_2) \right\}, \quad (16)$$

where

$$\Delta(2p \cdot q_1) = \frac{1}{\pi} \frac{\epsilon}{(2p \cdot q_1)^2 + \epsilon^2},$$

which approaches the Dirac delta function  $\delta(2p \cdot q_1)$  in the limit  $\epsilon \rightarrow 0$ .

We consider next the case of the (coherent) multiple collisions of a fast fermion with three fermion scatterers in the reaction  $p + a_a + a_2 + a_3 \rightarrow p' + a'_1 + a'_2 + a'_3$ . The Feynman diagrams for the multiple collisions process are shown in Fig. 2.

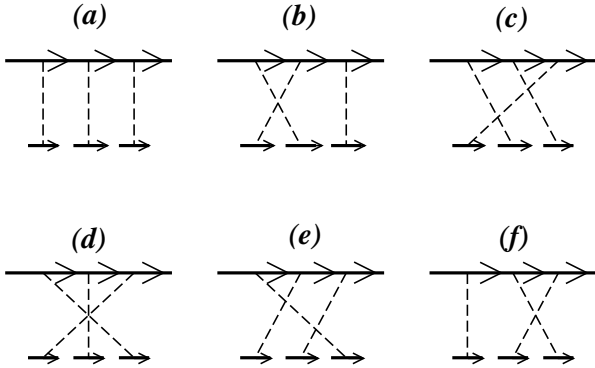


FIG. 2: Feynman diagrams for the multiple collisions of a fast fermion with three medium fermions in different permutations of the exchanged bosons.

In the high-energy limit, the Feynman amplitude for the collision is

$$M = \frac{g^6}{2m} \frac{2p \cdot \tilde{a}_1}{m_1} \frac{2p \cdot \tilde{a}_2}{m_2} \frac{2p \cdot \tilde{a}_3}{m_3} \frac{1}{q_1^2 q_2^2 q_3^2} \times \left\{ \left[ \frac{1}{(2p \cdot q_1 - i\epsilon)(2p \cdot q_1 + 2p \cdot q_2 - i\epsilon)} \right. \right.$$

$$\left. + \frac{1}{(2p \cdot q_2 - i\epsilon)(2p \cdot q_1 + 2p \cdot q_2 - i\epsilon)} \right] + \left[ \frac{1}{(2p \cdot q_2 - i\epsilon)(2p \cdot q_2 + 2p \cdot q_3 - i\epsilon)} + \frac{1}{(2p \cdot q_3 - i\epsilon)(2p \cdot q_2 + 2p \cdot q_3 - i\epsilon)} \right] + \left[ \frac{1}{(2p \cdot q_3 - i\epsilon)(2p \cdot q_3 + 2p \cdot q_1 - i\epsilon)} + \frac{1}{(2p \cdot q_1 - i\epsilon)(2p \cdot q_3 + 2p \cdot q_1 - i\epsilon)} \right] \}. \quad (17)$$

Each amplitude term in the curly bracket contains a distribution that is non-zero in various regions of  $p \cdot q_i$ . These Feynman amplitudes interfere among themselves. We can write Eq. (17) in the form

$$M = \frac{g^6}{2m} \left\{ \prod_{i=1}^3 \frac{2p \cdot \tilde{a}_i}{m_i q_i^2} \right\} \left\{ \prod_{j=1}^2 \frac{1}{\sum_{i=1}^j 2p \cdot q_i - i\epsilon} + \text{symmetric permutations} \right\}. \quad (18)$$

Generalizing to the case of the coherent collision of a fast fermion with  $n$  fermion scatterers in the process

$$p + a_1 + \dots + a_n \rightarrow p' + a'_1 + \dots + a'_n, \quad (19)$$

the total Feynman amplitude is

$$M = \frac{g^{2n}}{2m} \left\{ \prod_{i=1}^n \frac{2p \cdot \tilde{a}_i}{m_i q_i^2} \right\} \mathcal{M}(q_1, q_2, \dots, q_n), \quad (20)$$

where  $\mathcal{M}(q_1, q_2, \dots, q_n)$  is the sum of  $n!$  amplitudes involving symmetric permutations of the exchanged bosons given by

$$\mathcal{M}(q_1, q_2, \dots, q_n) = \prod_{j=1}^{n-1} \frac{1}{\sum_{i=1}^j 2p \cdot q_i - i\epsilon} + \text{symmetric permutations}. \quad (21)$$

The above sum involves extensive cancellations. Remarkably, it can be shown that this sum of  $n!$  symmetric permutations turns out to be a product of sharp distributions centered at  $2p \cdot q_i \sim 0$  [84],

$$\mathcal{M}(q_1, q_2, \dots, q_n) \Delta\left(\sum_{i=1}^n 2p \cdot q_i\right) = (2\pi i)^{n-1} \prod_{i=1}^n \Delta(2p \cdot q_i), \quad (22)$$

which gives

$$\mathcal{M}(q_1, q_2, \dots, q_n) = \frac{(2\pi i)^{n-1}}{n} \sum_{i=1}^n \left( \prod_{j=1, j \neq i}^n \Delta(2p \cdot q_j) \right). \quad (23)$$

Eqs. (21)-(23) indicate that for coherent collisions, there is a destructive interference of the Feynman amplitudes, leading to a cancellation in most regions of the phase

space. However there is a constructive interference in some other regions of the phase space, leading to sharp distributions at  $2p \cdot q_i \sim 0$ . The constraint  $\Delta(2p \cdot q_i)$  is mathematically the same as the constraint  $\Delta((p - q_i) - m^2)$  in the high-energy limit, which can be interpreted as the intermediate state  $p_{i+1} = (p - q_i)$  to be on the mass shell. It should however be kept in mind that the intermediate state  $p_{i+1} = (p - q_i)$  in the constraint of Eqs. (20), (22), and (23) is not a single particle but a quasi-particles that is the result of the interference of many amplitudes.

Equations (20)-(23) for the total Feynman amplitude for a coherent collision as a product of delta functions of  $2p \cdot q_i$  are similar to previous results obtained for the emission of many real photons or gluons in bremsstrahlung, and for the sum of ladder and cross-ladder amplitudes in the collision of two fermions [84]-[90].

#### IV. CROSS SECTION FOR (1+n)-BODY COLLISION

We wish to obtain the cross section for the coherent collision of a fast fermion  $p$  on  $n$  fermions  $\{a_1, a_2, a_3, \dots, a_n\}$  in reaction (19). While the Feynman rules to construct the Feynman amplitude are well known, the differential cross section for the reaction (19) as a single (1+n)-body collision process, written in terms of the Feynman amplitude  $M$ , does not seem to be available in the literature. We would like to examine the cross section rules in some details in this section.

It should be mentioned that the cross section rules for the (1+n)-body collision depend on the Feynman rules for the Feynman amplitude  $M$ . We shall use the Feynman rules of Refs. [84, 96] for  $M$ , which adopt the normalization  $\bar{u}u = 1$  for the fermion wave function. A different normalization of the fermion wave function according to  $\bar{u}u = 2m$ , as given in Ref. [97], will lead to slightly different cross section rules.

To be concrete, we use the auxiliary variable  $p_i$  with  $i = 1, \dots, n$  to label the intermediate state (or quasi-particle) of the incident fermion prior to its exchange of a virtual boson with scatterer  $a_i$  (or after its exchange of a virtual gluon with scatterer  $a_{i-1}$ ), with the special case  $p_1 = p$  and  $p_{n+1} = p'$ . The differential cross section for the collision process (19) involving (1+n) fermions is given by

$$d^n \sigma = \frac{|M|^2 (2\pi)^4 \delta^4 \{p + \sum_{i=1}^n a_i - p' - \sum_{i=1}^n a'_i\}}{\{\prod_{i=1}^n f_{pi}\} \{\prod_{i=2}^n (m/p_{i0})\} \{\prod_{i=2}^n T_i\}} \times \frac{d^4 p' 2m}{(2\pi)^3} \frac{D_{p'}(p')}{2p'_0} \left\{ \prod_{i=1}^n \frac{d^4 a'_i 2m_i}{(2\pi)^3} \frac{D_i(a'_i)}{2a_{i0}} \right\}, \quad (24)$$

where  $M$  is the total Feynman amplitude as follows from the Feynman rules of Refs. [84, 95, 96]. The quantity  $f_{pi}$  is the flux factor for a two-body collision between  $p_i$  and

the scatterer  $a_i$  of rest mass  $m_i$ ,

$$f_{pi} = \frac{4\sqrt{(p_i \cdot a_i)^2 - (m_i m_{iT})^2}}{(2m)(2m_i)}, \quad (25)$$

and  $m_{iT} = \sqrt{m_i^2 + \mathbf{a}_{iT}^2}$ .

In Eq. (24) we construct the flux factor for the (1+n)-body collision by requiring that it should be the same for all scatterers. Hence, it is the product of flux factors from all scatterers,  $\prod_{i=1}^n f_{pi}$ . We also need to require that in this flux factor, the momentum of the incident fermion and the scatterer fermions appear in the same power. Thus, the flux factor need to be linear in the energy of the colliding particles. But the product of  $\prod_{i=1}^n f_{pi}$  gives  $\prod_{i=1}^n p_{i0}$ . It is therefore necessary to multiply  $\prod_{i=1}^n f_{pi}$  by the factor  $\prod_{i=2}^n (m/p_{i0})$  to get the flux factor for the (1+n)-body collision that is linear in the energy of all colliding particles, resulting in the factors as given in the cross section formula in Eq. (24).

The quantity  $T_i$ , with  $\{i = 2, \dots, n\}$  is the collision time or the mean lifetime of the intermediate state (or quasi-particle)  $p_i$  of the incident fast particle prior to the incident particle exchanging a virtual boson with  $a_i$  (or after the incident particle has already exchanged of a virtual gluon with scatterer  $a_{i-1}$ ). It arises in the cross section formula because the cross section is proportional to the transition rate per unit time of collision and thus depends on the lifetime of the intermediate state  $p_i$  of the projectile before it exchanges a virtual boson with the scatterer  $a_i$ . The precise value of  $T_i$  needs not concern us at this point as it will be canceled later by the delta function that specifies the energy-momentum constraint of the intermediate state  $p_i$ , evaluated at the condition of the constraint of the delta function.

The states of the incident particle  $p'$  and the medium scatterer  $i'$  after the collision can come in different forms. They can be described by the functions  $D_{p'}/2p'_0$  and  $D_i/2a'_{i0}$ . For example, the final fast particle  $p'$  resides outside the medium after the collisions without interactions. Its state can be adequately described as being nearly on the mass shell,

$$\frac{D_{p'}(p')}{2p'_0} \sim \frac{\delta(p'_0 - \sqrt{\mathbf{p}'^2 + m^2})}{2p'_0} = \delta(p'^2 - m^2). \quad (26)$$

It may subsequently break up as jet fragments in a collimated narrow cone, in accordance with a jet fragmentation function. We shall examine the states of the scatterers in the next section.

To show the validity of Eq. (24), we note first that it is clearly correct for the case of a two-body collision with  $n = 1$ , as given in Appendix A-3 of Ref. [96]. We would like to test whether it gives the correct result for the case of quasi-elastic collisions where the answer is known. Such a case of quasi-elastic collisions is described by the generalization of ladder diagrams of Fig. 1(a), and 2(a), with the incident particle nearly on the mass shell and  $q_{i0} \sim 0$ . The diagram can be effectively cut at the intermediate fermion lines, resulting in a sequence of  $n$

disjoint two-body collision diagrams, and the many-body cross section is just the product of  $n$  two-body collisions.

We would like to show that for the above quasi-elastic collision case the Feynman amplitude approach with the cross section rules of Eq. (24) also leads to the known result.

In the high energy limit, the Feynman amplitude for the ladder diagrams of Fig. 1(a), and 2(a) can be generalized for  $n$  scatterers as given by

$$M \sim -\frac{g^{2n}}{2m} \left\{ \prod_{i=1}^{n-1} \frac{2p_i \cdot \tilde{a}_i}{m_i q_i^2} \frac{1}{(p_{i+1}^2 - m^2) + i\epsilon} \right\} \frac{2p_n \cdot \tilde{a}_n}{m_n q_n^2}. \quad (27)$$

For quasi-elastic collisions with  $q_{i0} \sim 0$ , the incident particle is nearly on the mass shell with  $p_{i+1}^2 \sim m^2$ . As a consequence, the propagator represented by  $1/(p_{i+1}^2 - m^2 + i\epsilon)$  in the Feynman amplitude can be approximated by the pole term

$$\frac{1}{p_{i+1}^2 - m^2 + i\epsilon} \rightarrow -i\pi \Delta(p_{i+1}^2 - m^2). \quad (28)$$

The Feynman amplitude becomes

$$M \sim \frac{g^{2n}}{2m} \left\{ \prod_{i=1}^{n-1} \frac{2p_i \cdot \tilde{a}_i}{m_i q_i^2} i\pi \Delta(p_i^2 - m^2) \right\} \frac{2p' \cdot \tilde{a}_n}{m_n q_n^2}. \quad (29)$$

We substitute this Feynman amplitude in Eq. (24), and we obtain

$$\begin{aligned} d^n\sigma &= \frac{1}{\{\prod_{i=1}^n f_{pi}\} \{\prod_{i=2}^n (m/p_{i0}) T_i\}} \frac{g^{4n}}{(2m)^2} \\ &\times \left\{ \prod_{i=1}^{n-1} \frac{(2p_i \cdot \tilde{a}_i)^2}{m_i^2 q_i^4} \pi^2 [\Delta(p_i^2 - m^2)]^2 \frac{d^4 a'_i 2m_i}{(2\pi)^3} \frac{D_i(a'_i)}{2a_{i0}} \right\} \\ &\times \frac{(2p' \cdot \tilde{a}_n)^2}{m^2 q_n^4} (2\pi)^4 \delta^4 \left\{ p + \sum_{i=1}^n a_i - p' - \sum_{i=1}^n a'_i \right\} \\ &\times \frac{d^4 p' 2m}{(2\pi)^3} \frac{D_{p'}(p')}{2p'_0} \frac{d^4 a'_n 2m_n}{(2\pi)^3} \frac{D_n(a'_n)}{2a_{n0}}. \end{aligned} \quad (30)$$

On the other hand, for the two-body collision  $p_i + a_i \rightarrow p_{i+1} + a'_i$ , the Feynman amplitude is

$$M_{pi}^{2B} = \frac{g^2}{2m} \frac{2p_i \cdot \tilde{a}_i}{m_i q_i^2}. \quad (31)$$

Upon writing  $\Delta(p_{i+1}^2 - m^2)$  in terms of the mean lifetime  $T_{i+1} = 1/\Gamma_{i+1}$  of the intermediate state of  $p_{i+1}$ , we have

$$\Delta(p_{i+1}^2 - m^2) = \frac{\Gamma_i/(4\pi p_{(i+1)0})}{\left[ p_{(i+1)0} - \sqrt{p_{i+1}^2 + m^2} \right]^2 + \Gamma_{i+1}^2/4},$$

we get

$$|\Delta(p_{i+1}^2 - m^2)|^2 = \Delta(p_{i+1}^2 - m^2) \frac{1}{2p_{(i+1)0}} \frac{2T_{i+1}}{\pi}, \quad (32)$$

where the mean lifetime  $T_{i+1}$  cancels the corresponding factor in the denominator of Eq. (30). Using Eqs. (31) and (32) in Eq. (30), we obtain

$$\begin{aligned} d^n\sigma &= \prod_{i=1}^{n-1} \frac{|M_{pi}^{2B}|^2}{f_{pi}} (2m) 2\pi \Delta(p_{i+1}^2 - m^2) \frac{d^4 a'_i 2m_i}{(2\pi)^3} \frac{D_i(a'_i)}{2a_{i0}} \\ &\times \frac{|M_{pn}^{2B}|^2}{f_{pn}} (2\pi)^4 \delta^4(p' + \sum_{i=1}^n q_i - p) \\ &\times \frac{d^4 p' 2m}{(2\pi)^3} \frac{D_{p'}(p')}{2p'_0} \frac{d^4 a'_n 2m_n}{(2\pi)^3} \frac{D_n(a'_n)}{2a_{n0}}. \end{aligned} \quad (33)$$

Inserting the unity factor  $\prod_{i=1}^{n-1} \delta(p_i + a_i - p_{i+1} - a'_i) d^4 p_{i+1} = 1$  into the above equation and noting that the differential cross section for  $p_i + a_i \rightarrow p_{i+1} + a'_i$  is

$$\begin{aligned} d\sigma_{pi}^{2B} &= \frac{|M_{pi}^{2B}|^2}{f_{pi}} (2\pi)^4 \delta^4(p_i + a_i - p_{i+1} - a'_i) \\ &\times \frac{d^4 p_{i+1} 2m}{(2\pi)^3} \frac{D_{i+1}(p_{i+1})}{2p_{(i+1)0}} \frac{d^4 a'_i 2m_i}{(2\pi)^3} \frac{D_i(a'_i)}{2a_{i0}}, \end{aligned} \quad (34)$$

we can rewrite Eq. (33) as

$$d^n\sigma = \prod_{i=1}^n d\sigma_{pi}^{2B}, \quad (35)$$

which is the cross section for quasi-elastic collisions. This show that Eq. (24) gives the correct cross section for the case for which the answer is known. It can therefore be used for a general treatment for the cross section in terms of many-body Feynman amplitudes in the general case of coherent collisions.

Equation (24) exhibits explicitly the rules for the cross section for coherent collision of an incident fast fermion with  $n$  fermion scatterers. The other cases for incident gluons and gluon scatterers will be taken up in Section IX.

## V. CONSEQUENCES OF THE BE INTERFERENCE ON THE RECOIL OF FERMION SCATTERERS

The states of a medium scatterer after the collision can come in different forms. As it acquires a large amount of energy and momentum from the incident jet, the medium scatterer can be far off the mass shell and it may subsequently fragment into a cluster of on-mass-shell particles. For an incident jet of energy 10 GeV with scatterers in a medium, it is however unlikely that the final scatterers themselves be energetic enough or far off the mass shell to fragment as clusters. Far more likely is the case of the scatterer  $a'_i$  to acquire a fraction of the incident jet energy and momentum and become only slightly off the mass shell, with the degree of its being off-mass shell described by a width  $\Gamma_i$ . As the medium particles reside in



an interacting medium, it will be subject to the interactions of the medium before and after the collision. We can describe the mass-shell constraint for the of medium scatterer  $a'_i$  after the collision as

$$D_i(a'_i) = \frac{\Gamma_i/2\pi}{[a'_{i0} - \sqrt{(\mathbf{a}'_i - g_i \mathbf{A})^2 + (m_i + S)^2} + g_i A_0]^2 + \frac{\Gamma_i^2}{4}},$$

where  $A = \{\mathbf{A}, A_0\}$  and  $S$  are the vector and scalar mean fields experienced by the medium scatterer  $a'_i$  after the collision, respectively. As the mean fields and scatterer widths increase with medium density and are presumably quite large and dominant for a dense medium, we shall approximately represent  $D_i$  as an average constant that is only a weak function of  $a'_i$ . Other descriptions of  $D_i/2a'_{i0}$  for the states of the scatterers are also possible but may not be as general; they can be the subjects for future investigations.

We integrate over  $\delta(p' + \sum q_i - p)d^4 p'$  and change variables from  $a'_i$  to  $q_i = a'_i - a_i$ . Writing out the matrix  $M$  explicitly as in Eq. (20) and using the relations in Eq. (22) and (23), we obtain from Eqs. (24)

$$d^n \sigma = \frac{g^{4n}(2m)^{n-1}}{(2\pi)^{n+1}} \left\{ \prod_{i=1}^n \frac{D_i}{f_{ij}} \right\} \left\{ \prod_{i=1}^{n-1} \frac{|\Delta(2p \cdot q_i)|^2 dq_{i0}}{(m/p_{(i+1)0})T_{i+1}} \right\} \\ \times \Delta(2p \cdot q_n) dq_{n0} \left\{ \prod_{i=1}^n \frac{(2p \cdot \tilde{a}_i)^2}{m^2 2a'_{i0}} \frac{d\mathbf{q}_{iT} dq_{iz}}{q_i^4} \right\}, \quad (36)$$

where for simplicity, we have taken  $m_i = m$ . The distribution  $\Delta(p \cdot q_i)$  can be written as

$$\Delta(2p \cdot q_i) = \frac{1}{p_0 + p_z} \Delta(q_{i0} - q_{iz} - \zeta), \quad (37)$$

where  $\zeta$  is

$$\zeta = \frac{-(p_0 - p_z)(q_{i0} + q_{iz}) + 2\mathbf{p}_T \cdot \mathbf{q}_T}{p_0 + p_z}, \quad (38)$$

and the quantity  $\zeta$  approaches zero in the high-energy limit of large  $p_0$ . The function  $\Delta(q_{i0} - q_{iz} - \zeta)$  provides the constraint at  $q_{i0} - q_{iz} \sim 0$ . As a consequence of the constraint, the integration  $\Delta(q_{i0} - q_{iz} - \zeta) dq_{i0}$  can be carried out, yielding

$$\int \Delta(2p \cdot q_i) dq_{i0} = \int \frac{1}{p_z + p_0} \Delta(q_{i0} - q_{iz} + \zeta) dq_{i0} = \frac{1}{2p_z}. \quad (39)$$

Noting that  $\Delta(2p \cdot q_i) \sim (p \cdot q_i)^2 m^2$ , we can express  $\Delta(2p \cdot q_i)$  in terms of the mean lifetime  $T_{i+1} = 1/\Gamma_{i+1}$  of the intermediate state  $p - q_i = p_{i+1}$  of the fast projectile, after it has exchanged of a virtual boson with the scatterer  $i$ , as

$$\Delta(2p \cdot q_i) = \frac{\Gamma_{i+1}/4\pi p_{(i+1)0}}{[p_{(i+1)0} - \sqrt{\mathbf{p}_{(i+1)}^2 + m^2}]^2 + \Gamma_{i+1}^2/4}. \quad (40)$$

then we have

$$|\Delta(2p \cdot q_i)|^2 = \Delta(2p \cdot q_i) \frac{T_{i+1}}{\pi p_{(i+1)0}}. \quad (41)$$

The above mean lifetime  $T_{i+1}$  cancels the mean lifetime  $T_i$  in the denominator of Eq. (36). The boson propagator  $q_i^2$  in the denominator becomes

$$q_i^2 = (q_{i0} + q_{iz})(q_{i0} - q_{iz}) - |\mathbf{q}_{iT}|^2 \approx -|\mathbf{q}_{iT}|^2. \quad (42)$$

We obtain

$$d^n \sigma = \frac{1}{4} \left( \frac{\alpha^2}{mp_z} \right)^n \left\{ \prod_{i=1}^n \frac{8D_i}{f_{pi}} \frac{(2p \cdot \tilde{a}_i)^2}{m^2 a'_{i0}} \frac{dq_{iz} d\mathbf{q}_{iT}}{|\mathbf{q}_T|^4} \right\} \quad (43)$$

where  $\alpha = g^2/4\pi$ . The last factor in the curly bracket is dimensionless, and  $d^n \sigma$  has the dimension of  $(\alpha^2/mp_z)^n$ , as it should be.

To find the probability distribution for the longitudinal momentum transfer  $q_{iz}$ , we introduce the fractional longitudinal momentum kick

$$x_i = \frac{q_{iz}}{p_z}, \quad dq_{iz} = p_z dx_i. \quad (44)$$

To investigate the  $x_i$  dependence of the factor  $(2p \cdot \tilde{a}_i)^2/2a'_{i0}$  in Eq. (43), we note from Eq. (11) that  $\tilde{a}_i$  can be written as a function of  $q_i$  and  $a_i$ ,

$$\tilde{a}_i \sim \sqrt{\frac{a_{i0} + m}{a'_{i0} + m}} \frac{q_i}{2} + \frac{a'_{i0} + m + a_{i0} + m}{\sqrt{(a'_{i0} + m)(a_{i0} + m)}} \frac{a_i}{2}. \quad (45)$$

Because of the  $\Delta(2p \cdot q_i)$  constraint, the factor  $(2p \cdot \tilde{a}_i)^2/2a'_{i0}$  in Eq. (43) becomes

$$\frac{(2p \cdot \tilde{a}_i)^2}{2a'_{i0}} \sim \frac{(a'_{i0} + a_{i0})^2}{2(a'_{i0})^2} \frac{(p \cdot a_i)^2}{a_{i0}} \equiv \kappa_i \frac{(p \cdot a_i)^2}{a_{i0}}. \quad (46)$$

We obtain from Eq. (43)

$$d^n \sigma = \left\{ \frac{1}{4} \left( \frac{\alpha^2}{m} \right)^n \left( \prod_{i=1}^n \frac{8D_i}{f_{ij}} \frac{\kappa_i (p \cdot a_i)^2}{ma_{i0}} \right) \right\} \\ \times \frac{dx_1 dx_2 \dots dx_n d\mathbf{q}_{1T} d\mathbf{q}_{2T} \dots d\mathbf{q}_{nT}}{|\mathbf{q}_{1T}|^4 |\mathbf{q}_{2T}|^4 \dots |\mathbf{q}_{nT}|^4}. \quad (47)$$

The fermion scatterers can possess different initial energies  $a_{i0}$  at the moment of their collisions with the energetic jet. In the case when  $a_{i0} \ll q_{i0}$ , the factor  $\kappa_i$  approaches  $1/2 + O(a_{i0}/q_{iz})$  with  $(a_{i0}/q_{iz}) \ll 1$ . In the other extreme when  $a_{i0} \gg q_{i0}$ , the factor  $\kappa$  approaches  $2 + O(q_{iz}/a_{i0})$  with  $(q_{iz}/a_{i0}) \ll 1$ . The dependence of  $\kappa_i$  on  $x_i$  and  $\mathbf{q}_{iT}$  is weak in either limits, and such dependencies can be neglected in our approximate estimate. We obtain then

$$d^n \sigma \sim C_q \frac{dx_1 dx_2 \dots dx_n d\mathbf{q}_{1T} d\mathbf{q}_{2T} \dots d\mathbf{q}_{nT}}{|\mathbf{q}_{1T}|^4 |\mathbf{q}_{2T}|^4 \dots |\mathbf{q}_{nT}|^4}, \quad (48)$$

where  $C_q$  is

$$C_q = \left\{ \frac{1}{4} \left( \frac{\alpha^2}{m} \right)^n \left( \prod_{i=1}^n \frac{8D_i}{f_{ij}} \frac{\kappa_i (p \cdot a_i)^2}{ma_{i0}} \right) \right\}, \quad (49)$$

the quantity  $C_q$  is a weak function of  $x_i$  and  $\mathbf{q}_{iT}$  and can be approximated as a constant.

By symmetry, the fraction of momentum transfers  $x_i$  for different scatterers should be approximately the same on the average, and  $x_i^{\max} \sim 1/n$ . Then as far as  $x_i$  is concerned, the average distribution is

$$\frac{dP}{dx_i} \sim n \Theta\left(\frac{1}{n} - x_i\right), \quad (50)$$

and the average longitudinal momentum fraction is

$$\langle x_i \rangle \sim \frac{1}{2n} \quad \text{or} \quad \langle q_{iz} \rangle \sim \frac{p_z}{2n}. \quad (51)$$

The above result in Eq. (50) indicate that the probability distribution of the longitudinal momentum transfer of a scatterer is approximately flat in  $x_i$ . The quasi-elastic scattering with  $q_{iz} \sim 0$  occurs, but with about the same probability as other longitudinal momentum transfer up to  $q_{iz} = p_z/n$ . On the average, a scatterer acquires approximately  $1/2n$  fraction of the incident jet longitudinal momentum.

Because of the recoils of the scatterers, the incident jet loses its longitudinal momentum. On the average, the jet loses a longitudinal momentum fraction of  $1/2n$  after each collision with a scatterer. When the jet emerges out of the medium after colliding with  $n$  scatterers, the (average) fractional jet longitudinal momentum loss due to scatterers recoils is approximately

$$\begin{aligned} \langle \text{fractional jet longitudinal momentum loss} \rangle &\sim n \times \frac{1}{2n} \\ &= \frac{1}{2}. \end{aligned} \quad (52)$$

Having obtained the differential cross section Eq. (48), we can infer the distribution of the scatterers with respect to the incident particle axis. Equation (48) indicates that the reaction has a high probability for the occurrence of small values of  $|\mathbf{q}_{iT}|$ , in the passage of an energetic fermion making coherent collisions with medium partons. The singularities at  $|\mathbf{q}_{iT}| \sim 0$  in Eq. (48) correspond to the case of infrared instabilities that may be renormalized, and a momentum cut-off  $\Lambda_{\text{cut}}$  may be introduced. As  $\mathbf{q}_{iT}$  are independent degrees of freedom, Eq. (43) or (48) shows that the standard deviation of the transverse momentum distribution of the scattered incident particle is related to the transverse momentum transfers to the scatterers by

$$\langle (\mathbf{p}'_T)^2 \rangle = \langle \left( \sum_{i=1}^n \mathbf{q}_{iT} \right)^2 \rangle = \sum_{i=1}^n \langle \mathbf{q}_{iT}^2 \rangle = n \langle \mathbf{q}_{iT}^2 \rangle, \quad (53)$$

as in a random walk in the transverse direction.

Equations (48)-(51) indicate further that the scatterers acquire an average longitudinal momentum  $\langle q_{iz} \rangle \sim p_z/2n$  that is expected to be much greater than  $\langle |\mathbf{q}_{iT}| \rangle$ . Thus, in a coherent collision there is a collective quantum many-body effect arising from Bose-Einstein interference such

that the fermion scatterers emerge in the direction of the incident particle, each carrying a fraction of the forward longitudinal momentum of the incident particle that is inversely proportional to twice the number of scatterers,  $\langle q_{iz} \rangle \sim p_z/2n$ .

We have presented an explicit derivation of the differential cross section as a function of the momenta of the recoil scatterers by making many simplifying assumptions. The explicit derivation has the advantage that it allows future refinements on some parts of the calculation by modifying some of the simplifying assumptions.

## VI. BOSE-EINSTEIN INTERFERENCE FOR COLLISIONS IN NON-ABELIAN THEORY

The above considerations for the Abelian theory can be extended to the non-Abelian theory. As an example, we consider a quark jet  $p$  making coherent collisions with quarks  $a_1$  and  $a_2$  in the reaction  $p + a_1 + a_2 \rightarrow p' + a'_1 + a'_2$ , in the non-Abelian theory. We shall neglect four-particle vertices and loops, which are of higher-orders. The Feynman diagrams are then the same as those in Fig. 1. One associates each quark vertex with a color matrix  $T_{\alpha,\beta}^{(p,1,2)}$  where the superscript  $p, 1$ , or  $2$  identifies the quark  $p, a_1$ , or  $a_2$ , and the subscripts  $\alpha$  or  $\beta$  give the  $SU(3)$  color matrix index. The Feynman amplitude  $M_a$  for diagram 1(a) is

$$\begin{aligned} M_a &= -g^4 \bar{u}(\mathbf{p}') T_{\beta}^{(p)} \gamma_{\nu} \frac{1}{\not{p} - \not{q}_1 - m + i\epsilon'} T_{\alpha}^{(p)} \gamma_{\mu} u(\mathbf{p}) \\ &\times \frac{1}{q_2^2} \bar{u}(\mathbf{a}'_2) T_{\beta}^{(2)} \gamma_{\nu} u(\mathbf{a}_2) \frac{1}{q_1^2} \bar{u}(\mathbf{a}'_1) T_{\alpha}^{(1)} \gamma_{\mu} u(\mathbf{a}_1). \end{aligned}$$

The Feynman amplitude  $M_b$  for diagram 1(b) is

$$\begin{aligned} M_b &= -g^4 \bar{u}(\mathbf{p}') T_{\alpha}^{(p)} \gamma_{\mu} \frac{1}{\not{p} - \not{q}_2 - m + i\epsilon'} T_{\beta}^{(p)} \gamma_{\nu} u(\mathbf{p}) \\ &\times \frac{1}{q_2^2} \bar{u}(\mathbf{a}'_2) T_{\beta}^{(2)} \gamma_{\nu} u(\mathbf{a}_2) \frac{1}{q_1^2} \bar{u}(\mathbf{a}'_1) T_{\alpha}^{(1)} \gamma_{\mu} u(\mathbf{a}_1). \end{aligned}$$

In the high-energy limit for coherent collisions, the sum of the Feynman amplitudes is

$$\begin{aligned} M &\sim \frac{g^4}{2m} \frac{2p \cdot \tilde{a}_1}{m} \frac{2p \cdot \tilde{a}_2}{m} \frac{1}{q_2^2 q_1^2} \\ &\times \left( \frac{T_{\beta}^{(p)} T_{\alpha}^{(p)} T_{\beta}^{(2)} T_{\alpha}^{(1)}}{2p \cdot q_1 - i\epsilon} + \frac{T_{\alpha}^{(p)} T_{\beta}^{(p)} T_{\beta}^{(2)} T_{\alpha}^{(1)}}{2p \cdot q_2 - i\epsilon} \right). \end{aligned} \quad (54)$$

We can rewrite the product of the color matrices for the quark jet  $p$  as

$$T_{\beta}^{(p)} T_{\alpha}^{(p)} = \frac{1}{2} \left( [T_{\beta}^{(p)}, T_{\alpha}^{(p)}]_+ + [T_{\beta}^{(p)}, T_{\alpha}^{(p)}]_- \right), \quad (55)$$

$$T_{\alpha}^{(p)} T_{\beta}^{(p)} = \frac{1}{2} \left( [T_{\beta}^{(p)}, T_{\alpha}^{(p)}]_+ - [T_{\beta}^{(p)}, T_{\alpha}^{(p)}]_- \right). \quad (56)$$

We label the propagators in Eq. (54) as  $\mathcal{M}_a$  and  $\mathcal{M}_b$ ,

$$\mathcal{M}_a = \frac{1}{2p \cdot q_1 - i\epsilon}, \quad \text{and} \quad \mathcal{M}_b = \frac{1}{2p \cdot q_2 - i\epsilon}. \quad (57)$$

The Feynman amplitude for coherent collision is then

$$M \sim \frac{g^4}{2m} \frac{2p \cdot \tilde{a}_1}{m} \frac{2p \cdot \tilde{a}_2}{m} \frac{1}{q_2^2 q_1^2} \times \left\{ (\mathcal{M}_a + \mathcal{M}_b) \frac{[T_\beta^{(p)}, T_\alpha^{(p)}]_+ T_\beta^{(2)} T_\alpha^{(1)}}{2} + (\mathcal{M}_a - \mathcal{M}_b) \frac{[T_\beta^{(p)}, T_\alpha^{(p)}]_- T_\beta^{(2)} T_\alpha^{(1)}}{2} \right\}. \quad (58)$$

The first term inside the curly bracket has the same space-time structure as what one obtains in the Abelian theory. It is given by the Abelian Feynman amplitude in Section II, multiplied by the color factor

$$C_{CF} = \frac{T_\beta^{(2)} T_\alpha^{(1)}}{2} [T_\beta^{(p)}, T_\alpha^{(p)}]_+. \quad (59)$$

The sum of  $\mathcal{M}_a$  and  $\mathcal{M}_b$  leads to sharp distributions at  $p \cdot q_1 \sim 0$  and  $p \cdot q_2 \sim 0$ ,

$$\mathcal{M}_a + \mathcal{M}_b = i\Delta(2p \cdot q_1) + i\Delta(2p \cdot q_2). \quad (60)$$

The second term is new and occurs only in the non-Abelian theory, as it involves the commutator of  $T_b^{(p)}$  and  $T_a^{(p)}$ . It involves the difference of  $\mathcal{M}_a$  and  $\mathcal{M}_b$  in which the sharp distributions cancel each other, leaving a broad distribution,

$$\mathcal{M}_a - \mathcal{M}_b = \frac{4p \cdot q_1}{(2p \cdot q_1)^2 + \epsilon^2}. \quad (61)$$

From the above analysis, we find that the color degrees of freedom in QCD bring in additional properties to the Feynman amplitude. Bose-Einstein symmetry with respect to the interchange of gluons in QCD involves not only the space-time exchange symmetry but also color index exchange symmetry. The total exchange symmetry can be attained with symmetric space-time amplitudes and symmetric color index factors as in the first  $\mathcal{M}_a + \mathcal{M}_b$  term in Eq. (58). The total symmetry can also be attained with space-time antisymmetry and color index antisymmetry, as in the second  $\mathcal{M}_a - \mathcal{M}_b$  term in Eq. (58).

We consider next the case for the collision of a quark jet with three quark scatterers in the reaction  $p + a_a + a_2 + a_3 \rightarrow p' + a'_1 + a'_2 + a'_3$  in the non-Abelian theory. The Feynman diagrams for the collision process are the same as those in Fig. 2 where we associate the color matrices  $T_a^{(1)}, T_b^{(2)}, T_c^{(3)}$  of color indices  $a, b, c$  with fermion scatterers  $a_1, a_2$  and  $a_3$  respectively. In the high-energy limit, the Feynman amplitude for the collision is

$$M = \frac{g^6}{2m} \frac{2p \cdot \tilde{a}_1 2p \cdot \tilde{a}_2 2p \cdot \tilde{a}_3}{m^3 q_1^2 q_2^2 q_3^2} T_a^{(1)} T_b^{(2)} T_c^{(3)}$$

$$\times \left\{ T_a T_b T_c M_{123} + T_a T_c T_b M_{132} + T_b T_c T_a M_{231} + T_b T_a T_c M_{213} + T_c T_a T_b M_{312} + T_c T_b T_a M_{321} \right\} \quad (62)$$

where  $T_{a,b,c}$  without a superscript are the color matrices for the incident quark jet  $p$ , and the amplitudes  $M_{123}, M_{132}, M_{231}, M_{213}, M_{312}, M_{321}$  are sequentially the six terms in the curly brackets of the Abelian Feynman amplitudes in Eq. (17). It is easy to show that the quantity in the curly bracket of Eq. (62) can be re-written as

$$\begin{aligned} \mathcal{M} = & \{T_a[T_b, T_c]_+ + T_b[T_c, T_a]_+ + T_c[T_a, T_b]_+\} \\ & \times [M_{123} + M_{132} + M_{231} + M_{213} + M_{312} + M_{321}]/2 \\ & - T_a[T_b, T_c]_+ [M_{231} + M_{213} + M_{312} + M_{321}]/2 \\ & - T_b[T_c, T_a]_+ [M_{123} + M_{132} + M_{312} + M_{321}]/2 \\ & - T_c[T_a, T_b]_+ [M_{123} + M_{132} + M_{231} + M_{213}]/2 \\ & + T_a[T_b, T_c]_- (M_{123} - M_{132})/2 \\ & + T_b[T_c, T_a]_- (M_{231} - M_{213})/2 \\ & + T_c[T_a, T_b]_- (M_{312} - M_{321})/2. \end{aligned} \quad (63)$$

The first term on the right hand side involves the symmetric sum of the space-time part of permuted amplitudes as in the Abelian case, multiplied by the symmetric permutation of the color indices. It yields a Feynman amplitude that is just the Abelian Feynman amplitude multiplied by the color factor

$$C_{CF} = \frac{T_a^{(1)} T_b^{(2)} T_c^{(3)}}{2} \left\{ T_a[T_b, T_c]_+ + T_b[T_c, T_a]_+ + T_c[T_a, T_b]_+ \right\}.$$

The other terms involve partial symmetry and antisymmetry with respect to the exchange of color indices. Similar studies on the collision of a jet with  $n$  partons can be carried out as in [83–90]. For our present work, it suffices to note that there will always be a component of the Feynman amplitude that is symmetric under both space-time exchange and color index exchange involving the sum of all space-time amplitude components, similar to the  $\mathcal{M}_a + \mathcal{M}_b$  sum in Eq. (58) and the first term on the right-hand side of Eq. (63). There will also be other space-time antisymmetric and color index exchange antisymmetric components.

For the space-time symmetric and color index exchange symmetric component, the Feynman amplitude is equal to the Abelian Feynman amplitude multiplied by a color factor. It will exhibit the same degree of Bose-Einstein interference as in the Abelian theory. Previous analysis on the longitudinal momentum transfer of recoiling fermions in the Abelian theory in Section 2 can be applied for the non-Abelian theory for this space-time symmetric and color index exchange symmetric component. There is thus a finite probability for the presence of delta function constraints to lead to recoiling quarks receiving significant moment kicks along the direction of the incident quark jet.

## VII. COLLISION OF A GLUON JET WITH QUARK SCATTERERS

It is of interest to generalize the above considerations to the coherent multiple collisions of a gluon jet. We shall neglect four-particle vertices and loops, which are of higher-orders. The Feynman diagrams for the collision of a gluon jet with medium quarks or medium gluons then have structures and momentum flows the same as those in the collision of a quark jet with quark scatterers. In the high-energy limit, the propagators and the three-particle vertices have approximately the same momentum dependencies, and the Bose-Einstein symmetry with respect to the interchange of the virtual bosons is the same. One expects that aside from the presence of color factors and color indices, the results for the Bose-Einstein interference in collisions with a gluon jet or a quark jet should be similar. This is so because the high-energy processes are insensitive to the spins of the colliding particles, as the current carried by a high energy particle is dominated by its center-of-mass motion, much more so than its spin current [86, 98, 99].

It is instructive to study the coherent collision of a fast gluon  $p$  with two quarks in non-Abelian gauge field theories in the reaction  $p + a_1 + a_2 \rightarrow p' + a'_1 + a'_2$  as an examples of the type of BE interference for the collision of a gluon jet. The collision process is represented by the two Feynman diagrams in Fig. 3.

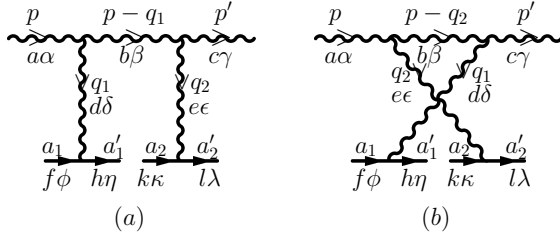


FIG. 3: Feynman diagrams for the collision of a gluon jet  $p$  with quark partons  $a_1, a_2$  with the momentum transfers  $q_1$  and  $q_2$  in the reaction  $p + a_1 + a_2 \rightarrow p' + a'_1 + a'_2$ . Here,  $\{a, b, c, \dots, k, l\}$  label the color states and  $\{\alpha, \beta, \dots, \eta, \lambda\}$  label the momentum components of various particles.

We consider the Feynman amplitude matrix element between the initial three particle state  $|pa\alpha, a_1 f\phi, a_2 k\kappa\rangle$  and the final state  $|p'c\gamma, a'_1 h\eta, a'_2 l\lambda\rangle$  where  $\{a, f, k, c, h, l\}$  label the color states and  $\{\alpha, \phi, \kappa, \gamma, \eta, \lambda\}$  label components of various particle currents. Using the Feynman rules and the overall phase factors as given in Ref. [84], the Feynman amplitude matrix element of Fig. 3(a) is given by

$$\begin{aligned} & \langle p'c\gamma, a'_1 h\eta, a'_2 l\lambda | M_a | pa\alpha, a_1 f\phi, a_2 k\kappa \rangle \\ &= g^4 \frac{f_{bec} f_{bad}}{q_1^2 q_2^2 (2p \cdot q_1 - i\epsilon)} (T_e^{(2)})_{lk} (T_d^{(1)})_{hf} \epsilon_\gamma(p') \\ & \times \{g_{\gamma\beta}(p' + p - q_1)_\epsilon + g_{\beta\epsilon}(-p + q_1 - q_2)_\gamma + g_{\epsilon\gamma}(q_2 - p')_\beta\} \\ & \times \{g_{\beta\alpha}(2p - q_1)_\delta + g_{\alpha\delta}(-p - q_1)_\beta + g_{\delta\beta}(2q_1 - p)_\alpha\} \epsilon_\alpha^*(p) \end{aligned}$$

$$\times \bar{u}(a'_2) \gamma_\epsilon u(a_2) \bar{u}(a'_1) \gamma_\delta u(a_1), \quad (64)$$

where  $\epsilon(p)$  and  $\epsilon(p')$  are the polarization vectors for gluons  $p$  or  $p'$  respectively. In the high-energy limit in which  $|p| \gg \{|q_i|, |a_i|, m\}$ , terms of order  $\{|q_i|/|p|, |a_i|/|p|, m/|p|\}$  in the three-gluon vertices can be neglected, and the helicities can be assumed to conserve. We then obtain

$$\begin{aligned} & \langle p'c\gamma, a'_1 h\eta, a'_2 l\lambda | M_a | pa\alpha, a_1 f\phi, a_2 k\kappa \rangle \\ &= g^4 \frac{(T_e^{(p)})_{cb} (T_d^{(p)})_{ba} (T_e^{(2)})_{lk} (T_d^{(1)})_{hf}}{q_1^2 q_2^2 (2p \cdot q_1 - i\epsilon)} \frac{2p \cdot \tilde{a}_1}{m} \frac{2p \cdot \tilde{a}_2}{m}, \end{aligned} \quad (65)$$

where the coefficients  $f_{bec}$  and  $f_{bad}$  in Eq. (64) have been expressed as matrix elements of matrices  $T_d^{(p)}$  and  $T_e^{(p)}$  of the incident gluon  $p$  (or  $p'$ ) between gluon color states [84],

$$(T_d^{(p)})_{ba} = i f_{dba}, \quad (66)$$

$$(T_e^{(p)})_{cb} = i f_{ecb}. \quad (67)$$

Equation (65) can be re-written in a matrix form as

$$M_a = g^4 \frac{2p \cdot \tilde{a}_1 2p \cdot \tilde{a}_2}{m^2 q_1^2 q_2^2} \frac{T_e^{(p)} T_d^{(p)} T_e^{(2)} T_d^{(1)}}{2p \cdot q_1 - i\epsilon}. \quad (68)$$

We can obtain a similar result for the Feynman amplitude for diagram 3(b) by permuting the vertices of the exchange bosons. As a consequence, the sum of the two Feynman amplitudes from Figs. 3(a) and 3(b) is given by

$$\begin{aligned} M &= g^4 \frac{2p \cdot \tilde{a}_1 2p \cdot \tilde{a}_2}{m^2 q_1^2 q_2^2} \\ & \times \left\{ \frac{T_e^{(p)} T_d^{(p)} T_e^{(2)} T_d^{(1)}}{2p \cdot q_1 - i\epsilon} + \frac{T_d^{(p)} T_e^{(p)} T_e^{(2)} T_d^{(1)}}{2p \cdot q_2 - i\epsilon} \right\}. \end{aligned} \quad (69)$$

We note that the above equation for the collision of a gluon jet is in the same form as Eq. (54) for the collision of a quark jet except with the modification that in the above equation for a gluon jet, the operator  $T^{(p)}$  has matrix elements between gluon color states whereas the operator  $T^{(p)}$  in Eq. (54) for the quark jet has matrix elements between quark color states. As in Eq. (54), we can likewise express the product of the color matrices as

$$T_b^{(p)} T_a^{(p)} = \frac{1}{2} \left( [T_b^{(p)}, T_a^{(p)}]_+ + [T_b^{(p)}, T_a^{(p)}]_- \right), \quad (70)$$

$$T_a^{(p)} T_b^{(p)} = \frac{1}{2} \left( [T_b^{(p)}, T_a^{(p)}]_+ - [T_b^{(p)}, T_a^{(p)}]_- \right). \quad (71)$$

The Feynman amplitude for a gluon jet is then

$$\begin{aligned} M &\sim g^4 \frac{2p \cdot \tilde{a}_1 2p \cdot \tilde{a}_2}{m^2 q_1^2 q_2^2} \\ & \times \left\{ (\mathcal{M}_a + \mathcal{M}_b) \frac{[T_b^{(p)}, T_a^{(p)}]_+ T_b^{(2)} T_a^{(1)}}{2} \right. \\ & \left. + (\mathcal{M}_a - \mathcal{M}_b) \frac{[T_b^{(p)}, T_a^{(p)}]_- T_b^{(2)} T_a^{(1)}}{2} \right\}. \end{aligned} \quad (72)$$



Therefore, in the collision of both a gluon or a quark jet with quarks, there will always be a component of the Feynman amplitude that is symmetric under both space-time exchange and color index exchange, involving the sum of all space-time amplitude components. The similarity is so close that previous results concerning a quark jet in collision with quark scatterers apply equally well to a gluon jet.

### VIII. COLLISION OF A GLUON JET WITH GLUON SCATTERERS

There is however a small difference in the coherent collisions of a jet with gluon scatterers. We can consider the collision of a fast gluon  $p$  with two gluon scatterers  $a_1$  and  $a_2$  as shown in Fig. 4.

The matrix element of the Feynman amplitude in Fig. 4(a) is given by

$$\begin{aligned} & \langle p'c\gamma, a'_1h\eta, a'_2l\lambda \mid M_a \mid pa\alpha, a_1f\phi, a_2k\kappa \rangle \\ &= \frac{g^4 f_{bec} f_{bad} f_{kle} f_{fhd}}{q_1^2 q_2^2 (2p \cdot q_1 - i\epsilon)} \epsilon_\gamma(p') \epsilon_\alpha^*(p) \epsilon_\lambda(a'_2) \epsilon_\kappa^*(a_2) \epsilon_\eta(a'_1) \epsilon_\phi^*(a_1) \\ & \times \{g_{\gamma\beta}(p' + p - q_1)_\epsilon + g_{\beta\epsilon}(-p + q_1 - q_2)_\gamma + g_{\epsilon\gamma}(q_2 - p')_\beta\} \\ & \times \{g_{\beta\alpha}(2p - q_1)_\delta + g_{\alpha\delta}(-p - q_1)_\beta + g_{\delta\beta}(2q_1 - p)_\alpha\} \\ & \times \{g_{\kappa\lambda}(-a_2 - a'_2)_\epsilon + g_{\lambda\epsilon}(a'_2 + q_2)_\kappa + g_{\epsilon\kappa}(-q_2 + a_2)_\lambda\} \\ & \times \{g_{\phi\eta}(-a_1 - a'_1)_\delta + g_{\eta\delta}(a'_1 + q_1)_\phi + g_{\delta\phi}(-q_1 + a_1)_\eta\}. \end{aligned} \quad (73)$$

In the high-energy limit in which  $|p| \gg \{|q_i|, |a_i|, m\}$  and the helicities can be assumed to conserve, we obtain

$$\begin{aligned} & \langle p'c\gamma, a'_1h\eta, a'_2l\lambda \mid M_a \mid pa\alpha, a_1f\phi, a_2k\kappa \rangle \\ &= g^4 \frac{(T_e^{(p)})_{cb} (T_d^{(p)})_{ba} (T_e^{(2)})_{lk} (T_d^{(1)})_{hf}}{q_1^2 q_2^2 (2p \cdot q_1 - i\epsilon)} 4p \cdot \bar{a}_1 4p \cdot \bar{a}_2 \end{aligned} \quad (74)$$

where

$$\bar{a}_i = \frac{a_i + a'_i}{2}. \quad (75)$$

We can obtain a similar result for the Feynman amplitude for diagram 4(b) by permuting the vertices of the exchange bosons. As a consequence, the sum of the two Feynman amplitudes from Figs. 4(a) and 4(b) is given by

$$\begin{aligned} M &= g^4 \frac{4p \cdot \bar{a}_1 4p \cdot \bar{a}_2}{q_1^2 q_2^2} \\ & \times \left\{ \frac{T_e^{(p)} T_d^{(p)} T_e^{(2)} T_d^{(1)}}{2p \cdot q_1 - i\epsilon} + \frac{T_d^{(p)} T_e^{(p)} T_e^{(2)} T_d^{(1)}}{2p \cdot q_2 - i\epsilon} \right\}. \end{aligned} \quad (76)$$

By comparing the results for a quark jet on quark scatterers [Eq. (54)] with those for a gluon jet on quark scatterers [Eq. 69] or on gluon scatterers [Eq. (76)], we obtain the following simple rules to obtain from the results of quark jet on quark scatterers of Eq. (54) to those involving gluons: (1) provide an overall multiplicative factor of  $2m$  when a quark is replaced by a gluon, (2) keep

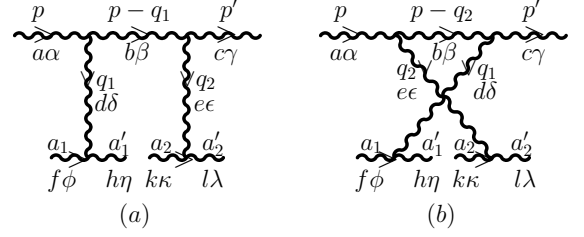


FIG. 4: Feynman diagrams for the interaction of a gluon jet  $p$  with gluon scatterers  $a_1, a_2$  with the momentum transfers  $q_1$  and  $q_2$ . Here,  $\{a, b, c, \dots, k, l\}$  label the color states and  $\{\alpha, \beta, \dots, \eta, \lambda\}$  label the momentum components of various particles.

the same form of the color operators, with the color operators that operate on the quark color states switched to operate on the gluon color states, and (3) change the momentum variable  $\bar{a}_i$  of Eq. (11) for a quark scatterer to  $\bar{a}_i$  of Eq. (75) for a gluon scatterer when a quark scatterer is replaced by a gluon scatterer. The above Rule (1) and (2) are well known results that were obtained previously on page 198 of Ref. [84]. Rule (3) is for our case in the collision with quark or gluon scatterers.

For completeness, we can use these rules to obtain the Feynman amplitude for the collision of a quark jet with two gluon scatterers as

$$\begin{aligned} M &= \frac{g^4}{2m} \frac{4p \cdot \bar{a}_1 4p \cdot \bar{a}_2}{q_1^2 q_2^2} \\ & \times \left\{ \frac{T_e^{(p)} T_d^{(p)} T_e^{(2)} T_d^{(1)}}{2p \cdot q_1 - i\epsilon} + \frac{T_d^{(p)} T_e^{(p)} T_e^{(2)} T_d^{(1)}}{2p \cdot q_2 - i\epsilon} \right\}. \end{aligned} \quad (77)$$

### IX. LONGITUDINAL MOMENTUM TRANSFER FOR GLUONS SCATTERERS

The cross section rules for Eq. (30) has been written for the collision of involving fermions (or quarks). The cross section rule involving incident gluons and/or gluon scatterers can be generalized by the rule that in replacing a fermion with a gluon, the  $2m_{\text{fermion}}$  factor for a fermion is replaced by unity for a gluon. Thus, we have explicitly the cross section formula for the coherent collision of an incident gluon with  $n$  fermion scatterers given by

$$\begin{aligned} d^n \sigma_{g+n f} &= \frac{|M|^2 (2\pi)^4 \delta^4 \{p + \sum_{i=1}^n a_i - p' - \sum_{i=1}^n a'_i\}}{\{\prod_{i=1}^n f_{pi}\} \{\prod_{i=2}^n (1/2p_{i0})\} \{\prod_{i=2}^n T_i\}} \\ & \times \frac{d^4 p'}{(2\pi)^3} \frac{D_{p'}(p')}{2p'_0} \left\{ \prod_{i=1}^n \frac{d^4 a'_i 2m_i}{(2\pi)^3} \frac{D_i(a'_i)}{2a_{i0}} \right\}, \end{aligned} \quad (78)$$

where

$$f_{pi}(\text{gluon on fermion}) = \frac{4p \cdot a_i}{2m_i}. \quad (79)$$

Similarly, the cross section formula for the coherent collision of an incident gluon with  $n$  gluon scatterers is given

by

$$d^n \sigma_{g+ng} = \frac{|M|^2 (2\pi)^4 \delta^4 \{p + \sum_{i=1}^n a_i - p' - \sum_{i=1}^n a'_i\}}{\{\prod_{i=1}^n f_{pi}\} \{\prod_{i=2}^n (1/2p_{i0})\} \{\prod_{i=2}^n T_i\}} \times \frac{d^4 p'}{(2\pi)^3} \frac{D_{p'}(p')}{2p'_0} \left\{ \prod_{i=1}^n \frac{d^4 a'_i}{(2\pi)^3} \frac{D_i(a'_i)}{2a_{i0}} \right\}, \quad (80)$$

where

$$f_{pi}(\text{gluon on gluon}) = 4p \cdot a_i. \quad (81)$$

The cross section formula for the coherent collision of an incident quark of rest mass  $m$  with  $n$  gluon scatterers is given by

$$d^n \sigma_{g+ng} = \frac{|M|^2 (2\pi)^4 \delta^4 \{p + \sum_{i=1}^n a_i - p' - \sum_{i=1}^n a'_i\}}{\{\prod_{i=1}^n f_{pi}\} \{\prod_{i=2}^n (m/p_{i0})\} \{\prod_{i=2}^n T_i\}} \times \frac{d^4 p'}{(2\pi)^3} \frac{D_{p'}(p')}{2p'_0} \left\{ \prod_{i=1}^n \frac{d^4 a'_i}{(2\pi)^3} \frac{D_i(a'_i)}{2a_{i0}} \right\}, \quad (82)$$

where

$$f_{pi}(\text{fermion on gluon}) = \frac{4p \cdot a_i}{2m}. \quad (83)$$

The results in the last section indicate that for the Feynman amplitude there is a modification from  $\tilde{a}$  of Eq. (11) for a quark scatterer to  $\bar{a}_i$  of Eq. (75) for a gluon scatterer, when a quark scatterer is replaced by a gluon scatterer. Such a modification brings with it a change in the longitudinal momentum distribution of the gluon scatterers which we shall examine in this section.

We consider the coherent multiple collisions of a gluon jet or a gluon jet on  $n$  gluons scatterers. From the results in Eq. (76), the cross section for the scattering in the space-time symmetric and color symmetric state is

$$d^n \sigma_{g,ng} = \frac{C_{CF}}{4} \left( \frac{2\alpha^2}{p_z} \right)^n \left\{ \prod_{i=1}^n \frac{16D_i}{f_{pi}} \frac{(2p \cdot \bar{a}_i)^2}{2a'_{i0}} \frac{dq_{iz} d\mathbf{q}_{iT}}{|\mathbf{q}_T|^4} \right\} \quad (84)$$

where  $C_{CF}$  is the color factor for the space-time symmetric and color symmetric component and

$$f_{pi} = 4p_i \cdot a_i. \quad (85)$$

To investigate the longitudinal distribution of the scatterers, we need to investigate the  $q_{iz}$  dependence of the factor  $(2p \cdot \bar{a}_i)^2$  in Eq. (84), which can be written as

$$(2p \cdot \bar{a}_i)^2 = [2p \cdot (2a_i + q_i)]^2. \quad (86)$$

Because of the  $\Delta(2p \cdot q_i)$  constraint, the above result gives

$$(2p \cdot \bar{a}_i)^2 \Delta(2p \cdot q_i) \sim (4p \cdot a_i)^2 \Delta(2p \cdot q_i), \quad (87)$$

where the factor  $(4p \cdot a_i)^2$  is independent of the longitudinal recoil  $q_{iz}$  of the scatterer. It is convenient to use

the transfer rapidity  $\xi_i$  to represent the longitudinal momentum transfer  $q_{iz}$ ,

$$q_{iz} = m_{gT} \sinh \xi_i, \quad (88)$$

$$a'_{i0} = \sqrt{m_{gT}^2 + (a_{iz} + m_{gT} \sinh \xi_i)^2}, \quad (89)$$

where for simplicity the final transverse masses of the scatterers are taken to be their average value  $m_{gT}$ . To make the problem simple, we can take  $a_{iz}$  to have its average value  $\langle a_{iz} \rangle$ , which is zero in the medium center-of-momentum frame. In that approximation, we obtain from Eqs. (88) and (89)

$$\frac{dq_{iz}}{a'_{i0}} \sim d\xi_i. \quad (90)$$

From Eq. (84), the cross section becomes

$$d^n \sigma \sim C_g \frac{d\xi_1 d\xi_2 \dots d\xi_n d\mathbf{q}_{1T} d\mathbf{q}_{2T} \dots d\mathbf{q}_{nT}}{|\mathbf{q}_{1T}|^4 |\mathbf{q}_{2T}|^4 \dots |\mathbf{q}_{nT}|^4}, \quad (91)$$

where  $C_g$  is

$$C_g = \frac{C_{CF}}{4} \left( \frac{2\alpha^2}{p_z} \right)^n \left\{ \prod_{i=1}^n \frac{16D_i}{f_{pi}} \frac{(2p \cdot \bar{a}_i)^2}{2} \right\}. \quad (92)$$

The quantity  $C_g$  is a weak function of  $\xi_i$  and  $\mathbf{q}_{iT}$  and can be approximated as a constant. The probability distribution is then a flat function of  $\xi_i$ . The transfer rapidly  $\xi_i$  has the upper limit

$$\xi_{i\max} = \cosh^{-1} \left\{ \frac{p_0}{nm_{gT}} \right\}. \quad (93)$$

Then as far as  $\xi_i$  is concerned, the average distribution is

$$\frac{dP}{d\xi_i} \sim \frac{1}{\xi_{i\max}} \Theta(\xi_{i\max} - \xi_i). \quad (94)$$

The average  $\langle q_{iz} \rangle$  is

$$\langle q_{iz} \rangle = \frac{p_0/n - m_{gT}}{\xi_{i\max}}. \quad (95)$$

With  $p_0 = 10$  GeV/c and  $m_{gT} = 0.6$  GeV, we find for  $n = 6$ ,

$$q_{iz} \sim 0.6 \text{ GeV/c}, \quad (96)$$

and for  $n = 2.4$ , we find

$$q_{iz} \sim 1.4 \text{ GeV/c}. \quad (97)$$

These estimates indicate that the average longitudinal momentum kick acquired by a gluon scatterer is slightly smaller than that acquired by a fermion scatterer. They are approximately inversely proportional to the number of scatterers in a coherent collision.

## X. SIGNATURES OF BOSE-EINSTEIN INTERFERENCE AND COMPARISON WITH EXPERIMENTAL DATA

The results in the above sections provide information on the signatures for the occurrence of the Bose-Einstein interference in the coherent collisions of a jet with medium partons:

1. The Bose-Einstein interference is a quantum many-body effect. It occurs only in the multiple collisions of the fast jet with two or more scatterers. Therefore there is a threshold corresponding to the requirement of two or more scatterers in the multiple collisions,  $n \geq 2$ .
2. Each scatterer has a transverse momentum distribution of the type  $1/|q_T|^4$ , which peaks at small values of  $|q_T|$ .
3. Each scatterer acquires a longitudinal momentum kick that is of order  $1/2n$  fraction of the incident jet momentum along the incident jet direction.
4. As a consequence, the final effect is the occurrence of collective recoils of the scatterers along the jet direction.

To inquire whether Bose-Einstein interference may correspond to any observable physical phenomenon, it is necessary to identify the scatterers to separate them from the incident jet in a measurement. Such a separation is indeed possible in  $\Delta\phi$ - $\Delta\eta$  angular correlation measurements of produced pairs with a high- $p_T$  trigger [1]-[30]. Particles in the “ridge” part of the correlations with  $|\Delta\eta| > 0.6$  at RHIC and  $|\Delta\eta| > 1.0$  at LHC with  $\Delta\phi \sim 0$  can be identified as belonging to the medium partons because it was observed at RHIC that

1. The yield of these ridge particles increases approximately linearly with the number of participants [3].
2. The yield of these ridge particles is nearly independent of (i) the flavor content, (ii) the meson/hyperon character, and (iii) the transverse momentum  $p_T$  (above 4 GeV) of the jet trigger [3, 4, 6].
3. The ridge particles have a temperature (inverse slope) that is similar (but slightly higher) than that of the inclusive bulk particles, but lower than the temperature of the near-side jet fragments [3].
4. The baryon/meson ratio of these ridge particles is similar to those of the bulk hadrons and is quite different from those in the jet fragments [19].

With the scatterers as ridge particles that can be separated from the incident high- $p_T$  jet, the occurrence of the Bose-Einstein interference will be signaled by Item (4) of the collective recoils of the scatterers (the ridge particles) along the jet direction. Such collective recoils will lead

to the  $\Delta\phi \sim 0$  correlation of the ridge particles with the high- $p_T$  trigger, as has been observed in angular correlations of produced hadrons in AuAu collisions at RHIC [1]-[23], and in pp and PbPb collisions at LHC [26-30]. The collective recoils of the kicked medium partons have been encoded into the longitudinal momentum kick  $\langle q_{iz} \rangle$  of the momentum kick model that yields the observed  $\Delta\phi$ ,  $\Delta\eta$ , and  $p_T$  dependencies of the angular correlations in AuAu collisions at RHIC [31-37], and pp collisions at LHC [38].

It is of interest to examine Item (3) of the signature of the Bose-Einstein interference with regarding to the relationship between the (average) magnitude of the longitudinal momentum kick,  $\langle q_{iz} \rangle$ , and the (average) number of scatterers,  $\langle n \rangle$ , when such a collective momentum kick occurs. For the most central AuAu collisions at  $\sqrt{s_{NN}} = 200$  GeV at RHIC, we previously found that  $\langle f_R \rangle \langle n \rangle \sim 3.8$  where  $n$  is the number of kicked medium partons and  $\langle f_R \rangle$  is the average attenuation factor for the kicked partons to emerge from the collision zone [33]. The value of  $\langle f_R \rangle$  is not determined but a similar attenuation factor  $\langle f_J \rangle$  for jet fragments is of order 0.63 [33]. We can therefore estimate that for the most central AuAu collisions at  $\sqrt{s_{NN}} = 200$  GeV at RHIC,  $\langle n \rangle \sim 6$ . For an incident jet of  $p_z \sim 10$  GeV/c [20], the estimates of Eq. (51) and (72) give

$$q_{iz} \sim \begin{cases} 0.83 \text{ GeV/c} & \text{for a quark scatterer,} \\ 0.63 \text{ GeV/c} & \text{for a gluon scatterer.} \end{cases} \quad (98)$$

These estimates of the momentum kick are of the same order as the value of  $\langle q_{iz} \rangle \sim 1$  GeV/c estimated in [33] and 0.8 GeV/c in [35], obtained in the momentum kick model analysis.

In another momentum kick model analysis for the highest multiplicity pp collisions at  $\sqrt{s_{NN}} = 7$  TeV at the LHC, we previously found that  $\langle f_R \rangle \langle n \rangle \sim 1.5$  [38]. The value of ridge particle attenuation factor  $\langle f_R \rangle$  is not determined but we can use again the similar attenuation factor for jet fragments,  $\langle f_J \rangle$  of order 0.63 [33], to estimate  $\langle n \rangle \sim 2.4$ . For an incident jet of 10 GeV/c, the estimates of Eqs. (51) and (95) give the average scatterer longitudinal recoil momentum as

$$q_{iz} \sim \begin{cases} 2.1 \text{ GeV/c} & \text{for a quark scatterer,} \\ 1.4 \text{ GeV/c} & \text{for a gluon scatterer.} \end{cases} \quad (99)$$

These estimates of the momentum kick are slightly lower than but are of the same order as of the same order as the value of  $\langle q_{iz} \rangle \sim 2$  GeV/c inferred from experimental data in the momentum kick model analysis [38]. The experimental data give a longitudinal momentum transfer that is approximately inverse proportional to the number of scatterers.

With regard to Item (1) for the signature for the occurrence of the Bose-Einstein interference, the presence of a threshold implies a sudden increase of the ridge yield as a function of the number of kicked medium scatterers,  $n$ , which increases with the increasing centrality, as represented either by an increasing number of participants

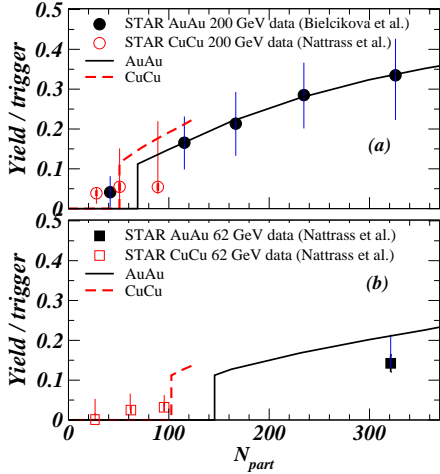


FIG. 5: (Color online) The ridge yield per high- $p_T$  trigger as a function of the participant number  $N_{\text{part}}$  for nucleus-nucleus collisions at  $\sqrt{s_{NN}}=200$  and 62 GeV. The solid circular points (for AuAu) and the square points (for CuCu) are from the STAR Collaboration [4, 10]. The curves are the momentum kick model results of [34] modified to include the Bose-Einstein interference threshold effect of  $n \geq 2$ .

or by increasing multiplicities. The slope of the yield as a function of centrality will change from zero below threshold to infinite over a small range of centralities at threshold. We expect that such a sudden threshold will be smoothed out by the fluctuations of the participant numbers and multiplicities with respect to the number of kicked medium partons. However the change of the slope of the ridge yield as a function of centralities will remain. Hence, the BE threshold effect will show up as a change of the slope of the ridge yield as a function of centralities, measured by the number of participants or by multiplicities. Equivalently, the ridge yield as a function of centralities will appear to have a kink near the threshold region of centrality. A search for a change of the slope or a kink in the ridge yield as a function of centralities will allow us to find the BE interference threshold.

We show in Fig. 5 the experimental ridge yield per high- $p_T$  trigger as a function of  $N_{\text{part}}$  for AuAu and CuCu collisions at  $\sqrt{s} = 200$  and 62 GeV at RHIC [4, 10]. We also show in Fig. 5 the theoretical yields obtained in the momentum kick model [33], where the ridge yield at the most central collision at  $N_{\text{part}} = 320$  was calibrated as  $n = 6$  [33]. With such a calibration, the threshold values in  $N_{\text{part}}$  at which  $n = 2$  can be located and listed in Table I, where the 30% theoretical errors arise from the errors in measuring the ridge yield at the most central collision at  $N_{\text{part}} = 320$ . Theoretical ridge yields from the momentum kick analysis in Fig. 10 of Ref. [33], modified to include the Bose-Einstein interference threshold effect of  $n \geq 2$ , are shown as the solid curves for AuAu collisions, and as dashed curves for CuCu collisions in Fig. 5. The theoretical thresholds in Fig. 5 will be smoothed out by the fluctuations of the number of scatterers as a

function of  $N_{\text{part}}$  and by uncertainties in the estimates of the number of scatterers. Although the experimental data appear to be consistent with theory, the large error bars and the scarcity of the number of data points in the threshold regions preclude a definitive conclusion.

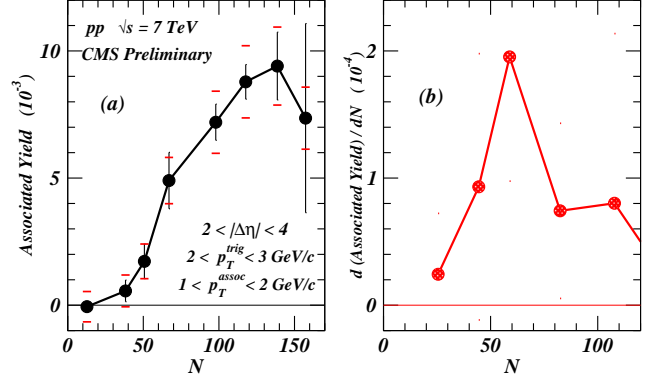


FIG. 6: (Color online) (a) Preliminary CMS Collaboration data of the ridge yield per trigger in the region of  $2 < |\Delta\eta| < 4$  for pp collisions at 7 TeV, for  $2 < p_T^{\text{trig}} < 3$  GeV/c,  $1 < p_T^{\text{assoc}} < 2$  GeV/c, as a function of multiplicities  $N$  [100]. (b) The slope of the ridge yield,  $d(\text{Associated Yield})/dN$  as a function of  $N$ .

In Fig. 6(a), we show the CMS preliminary data on the near-side ridge yield per trigger as a function of centralities, as measured by multiplicities  $N$ , for pp collisions at  $\sqrt{s}=7$  TeV [100]. To search for the BE threshold that may show up as a change of slope or a kink of the ridge yield as a function of multiplicities, we show the slope of the associated ridge yield,  $d(\text{Associated Yield})/dN$  as a function of  $N$  in Fig. 6(b). The lines in Fig. 6(a) and 6(b) join the data points to guide the eyes. The CMS preliminary data in Fig. 6(a) and 6(b) indicate a sharp change of the slope of the ridge yield in the region around  $N \sim 50 - 70$ , which may suggest a threshold for the ridge yield at around  $N = 50 - 70$ .

We show CMS preliminary data [100] on the near-side ridge yield per trigger for PbPb collision at  $\sqrt{s_{NN}}=2.76$  GeV/c as a function of the number of participants  $N_{\text{part}}$  in Fig. 7(a), and the corresponding  $d(\text{Associated Yield})/dN_{\text{part}}$  in Fig. 7(b). In Fig. 7, we also included the minimum-biased pp data point as an open circle for  $N_{\text{part}} = 2$  (for very peripheral PbPb collisions), at which the ridge yield is zero [26, 28]. The integrated near-side associated yield for  $4 < p_T^{\text{trig}} < 6$  GeV/c and  $2 < p_T^{\text{assoc}} < 4$  GeV in the ridge region of  $2 < |\Delta\eta| < 4$  appear to have a kink in the ridge yield as a function of  $N_{\text{part}}$  at  $\langle N_{\text{part}} \rangle \sim 30$  in Fig. 7(a). The slope increases sharply starting at  $N_{\text{part}} \sim 20$  in Fig. 7(b) and reaching a large value at  $N_{\text{part}} \sim 40$ . Such a behavior may suggest the presence of a ridge yield threshold. The location of a possible threshold at  $\langle N_{\text{part}} \rangle \sim 30$  for PbPb collisions appear to be qualitatively consistent with the decrease of  $\langle N_{\text{part}} \rangle$  as a function of increasing collision energies, as indicated in Table I. It will be of interest to examine in future work whether the ridge thresholds



as suggested by the CMS pp and PbPb data correspond quantitatively to the location of  $n = 2$  for the onset of the BE interference.

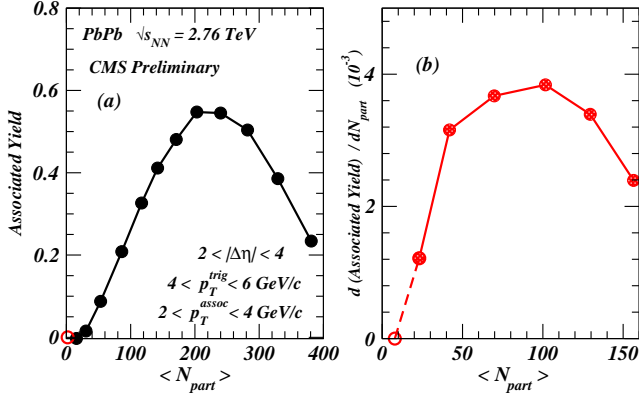


FIG. 7: Preliminary CMS data of the ridge yield per trigger in the ridge region of  $2 < |\Delta\eta| < 4$  for PbPb collisions at  $\sqrt{s_{NN}} = 2.76$  TeV, for  $4 < p_T^{\text{trig}} < 6$  GeV/c,  $2 < p_T^{\text{assoc}} < 4$  GeV/c, as a function of the number of participants  $N_{\text{part}}$ . [100].

Threshold effects for the ridge yield (2D Gaussian yield) as a function of  $N_{\text{part}}$  have been observed in another angular correlation measurements with a low- $p_T$  trigger from the STAR Collaboration [14–17] as shown in Fig. 8. We note previously that a fast jet parton possesses low- $p_T$  jet fragments and a minimum- $p_T$ -biased low- $p_T$  trigger can also indicate the passage of a fast parent jet [38]. As a consequence, ridge particles will also be associated with a low- $p_T$  trigger. The change of the slope of the amplitude of the 2D Gaussian distribution (the ridge yield) shown in Fig. 8 indicates the presence of a threshold for the ridge yield as a function of centrality.

TABLE I: Comparison of the locations of the theoretical threshold, at which the (average) number of scatterer  $n$  is equal to 2, with the observed experimental threshold [14–17] for the sudden increase of the 2D Gaussian distribution amplitude and width (ridge component) in AuAu collisions at  $\sqrt{s_{NN}} = 200$  and 62 GeV in Fig. 8.

Collision System	$\sqrt{s_{NN}}$ (GeV)	Theoretical Threshold $N_{\text{part}}$	Experimental Threshold $N_{\text{part}}$
AuAu	200	$69 \pm 21$	58-86
AuAu	62	$146 \pm 45$	85-122
CuCu	200	$51 \pm 15$	
CuCu	62	$103 \pm 31$	

For AuAu at 200 GeV/c, the experimental ridge yield threshold occurs at  $N_{\text{part}} = 58 - 86$  (Fig. 8), which can be compared in Table I with the theoretical ridge yield threshold of  $N_{\text{part}} = 69 \pm 21$  as estimated in the momentum kick model for  $n = 2$ . For AuAu at 62 GeV/c, the experimental ridge yield threshold occurs at  $N_{\text{part}} = 85 - 122$  (Fig. 8), which can be compared with the theoretical threshold of  $N_{\text{part}} = 146 \pm 45$  as estimated in the momentum kick model for  $n = 2$  (Table I).

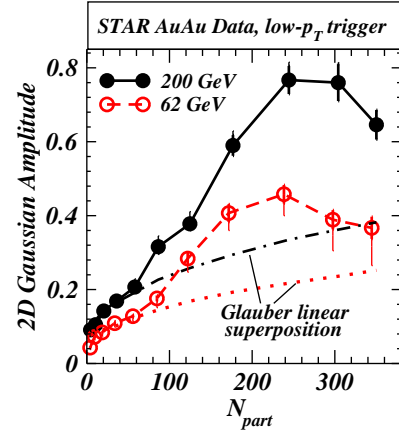


FIG. 8: (Color online) STAR Collaboration data of the 2D Gaussian distribution amplitude (ridge yield) for AuAu collisions at  $\sqrt{s_{NN}} = 200$  GeV (solid circles) and 62 GeV (open circles), with a low- $p_T$  trigger [14–17]. The solid and dashed curves are lines joining the data points. The dashed-dot and dotted curves represent Glauber linear superposition (GLS) estimates.

These comparisons indicate that experimental data with low- $p_T$  trigger are consistent with the presence of ridge thresholds as a function of the number of the medium scatterers located at  $n \sim 2$ , as in the threshold effect in Bose-Einstein interference.

## XI. CONCLUSIONS AND DISCUSSIONS

Conventional investigations [77–81, 91–94] on scattering of a fast particle with medium scatterers use the potential model in which the scatterers are represented by static potentials and the longitudinal recoils of the scatterers are considered as dependent variables that are appendages to the deflected motion of the incident particle. A general treatment of coherent collisions necessitates the use of the longitudinal recoils of the scatterers as independent dynamical variables which are however not allowed in the potential model. This leads us to forgo the potential model and to turn to the use of Feynman amplitudes for the general treatment of coherent collisions.

In the Feynman amplitude approach for the coherent collision of a fast particle on  $n$  scatterers, there are  $n!$  different orderings in the sequence of collisions along the fast particle trajectory at which various virtual bosons are exchanged. By Bose-Einstein symmetry, the total Feynman amplitude is the sum of the  $n!$  amplitudes for all possible interchanges of the virtual bosons. The summation of these  $n!$  Feynman amplitudes and the accompanying interference constitute the Bose-Einstein interference in the passage of the fast particle in the dense medium.

Our interest in examining this problem has been stimulated by the phenomenological successes of the momentum kick model in the analysis of the angular correlations of hadrons produced in high-energy heavy-ion collisions

[31–38]. We seek a theoretical foundation for the origin of the longitudinal momentum kick along the jet direction postulated in the model. We explore whether such a longitudinal momentum kick may originate from a quantum many-body effect arising from the Bose-Einstein interference in the passage of a jet in a dense medium. We take note of previous results on the Bose-Einstein interference in the emission of real photons and gluons in high-energy interactions and in the sum of the ladder and cross-ladder loop diagrams in the collision of two particles [83–90].

We find similarly that in the coherent collisions of an energetic fermion with  $n$  fermion scatterers at high energies in the Abelian theory, the symmetrization of the Feynman scattering amplitudes with respect to the interchange of the virtual bosons leads to the Bose-Einstein interference, resulting in a sharp distributions at  $p \cdot q_i \sim 0$ . Such coherent collisions are in fact a single collision, tying the incident fermion with the  $n$  fermion scatterers as a single unit. There are then  $3(n+1)$  degrees of freedom, subject to the constraints of the conservation of energy and momentum. As a consequence, all  $3n$  degrees of freedom of the scatterers can be independently varied. The probability distribution in these  $3n$  momentum degrees of freedom depends on the Feynman amplitudes and the phase-space factors. The Bose-Einstein symmetry constraints of  $p \cdot q_i \sim 0$  limit the transverse momentum transfers of the scatterers to small values of  $q_{iT}$ . The longitudinal momenta of the scatterers get their share of longitudinal momenta from the jet, resulting in the collective recoils of the scatterers along the jet direction.

For the coherent collision of an energetic parton with parton scatterers in non-Abelian cases, we find that the complete Bose-Einstein symmetry in the exchange of virtual gluons consists not only of space-time exchange symmetry but also color index exchange symmetry. Nevertheless, there is always a space-time symmetric and color-index symmetric component of the Feynman amplitude that behaves in the same way as the Feynman amplitude in the Abelian case, in addition to the occurrence of space-time antisymmetric and color-index antisymmetric components. For the space-time symmetric and color-index symmetric component, the recoiling partons behave in the same way as in collisions in the Abelian case. There is thus a finite probability for the parton scatterers to emerge collectively along the incident trigger jet direction, each with a significant fraction of the longitudinal momentum of the incident jet. The collective recoils will lead to the  $\Delta\phi \sim 0$  correlation of the ridge particles with the high- $p_T$  trigger. Such a signature of the Bose-Einstein interference may have been observed in the  $\Delta\phi \sim 0$  correlation of the ridge particles with a high- $p_T$  trigger in the angular correlation measurements of produced hadron pairs in AuAu collisions at RHIC [1]–[23] and in pp and PbPb collisions at LHC [26–30]. The centrality dependence of the ridge yields in pp and PbPb collisions at LHC with high  $p_T$  trigger [28, 100] and in AuAu collisions at RHIC with a low- $p_T$  trigger [14–17] gives hints of the presence of a ridge threshold,

as expected in the quantum many-body effect of Bose-Einstein interference.

Our focus at present is on the recoils of the scatterers. We have been examining the collision between the incident particle and the medium scatterers without radiation. We find that the scatterer recoils ranges from quasi-elastic to substantial fraction of the incident incident particle momentum. For a given multiple collision processes involving the recoils of the scatterers, the radiative processes will involve addition external legs in the Feynman diagram. They are high order in  $\alpha_s$ . Therefore as far as the cross sections are concerned, they generally occur with less probabilities. However, as far as jet energy loss is concerned, these high-order radiative processes can be important in certain kinematic regions. For example, if one restricts oneself to quasi-elastic processes with little scatterer longitudinal momentum recoils, then radiation can take up more of the jet longitudinal momentum, even though they occur with a lower probability than quasi-elastic scattering. One therefore envisages that in the investigation of the loss of the incident longitudinal momentum, radiative energy loss is important in the region of small scatterer longitudinal recoils, but the relative importance of the radiative energy loss will diminish as one moves toward the regions of greater scatterer longitudinal recoils.

If one restricts oneself to potential models, then the longitudinal momentum and energy losses due to scatterer recoils will be small and radiative energy loss becomes more important than quasi-elastic collision energy loss. However, for reasons we examine in Section II and discussed earlier in this section, the general treatment of coherent collisions necessitates the use of the longitudinal recoils of the scatterers as independent dynamical variables, which are however not allowed in the potential model. It is necessary to use the Feynman amplitude approach to explore the entire domain of longitudinal scatterers recoils. We hope to carry out an analysis of radiative processes in conjunction with scatterer recoils within the Feynman amplitude approach in the future.

The present work is based on the high-energy limit which allows great simplifications of the algebraic structures of Feynman amplitudes. These simplified structures bring into clear focus the mechanism of the Bose-Einstein interference that changes the nature of the distribution function. With the mechanism of the Bose-Einstein interference well understood, it may be beneficial in future work to evaluate the Feynman amplitudes without resorting to many of the drastic assumptions and simplifications – in order to make quantitative comparison of theoretical predictions with results of the longitudinal momentum kick quantities extracted from experimental data. This is particularly important in regions of large longitudinal momentum transfers for which the high-energy approximation of having  $p'$  not greatly different from  $p$  may not hold.

Coherence or decoherence in high energy processes occurs when the scattering amplitude consists of many con-

tributions and these contributing amplitudes interfere. Because of its general nature, they come in many different processes in different forms.

The coherence results we present here have been obtained for a single jet and interacting particles as plane waves. High-energy collisions has a preference for longitudinal motion over transverse motion. Therefore, for a single jet, as in the case of our main interest, the interference of Feynman diagrams has relevance only with regard to longitudinal coherence length along the longitudinal direction. For such a configuration, the uncertainties of the vertices of boson emission along the longitudinal direction leads to the coherence in the collision process. Uncertainties in the transverse direction come from the transverse positions of the scatterers. Such uncertainties can be included by treating the scatterers in terms of wave packets [101], form factors [102], or scatterer wave function [94]. In the special case of a purely elastic scattering of an incident fast particle with medium particles (in a nucleus), there can be constructive interference of the scattering amplitudes from different particles, leading to a sharp diffractive elastic peak at the forward angle, as described by Glauber [102].

However, there are circumstances in which interesting transverse uncertainties arises, and the amplitudes from different transverse sources interfere. An interesting case of transverse interference can be found in connection with the coherent emission of a gluon from a system of a quark jet and an antiquark jet [92, 93]. This case involves the propagation of two jets with an opening transverse angle  $\theta_{q\bar{q}}$  and differs from our present case with the propagation of a single jet. The amplitude for gluon emission from the quark  $q$  interfere with the amplitude for gluon emission from the antiquark  $\bar{q}$ . As a consequence, in the absence of medium, the coherent interference in the transverse direction lead to the angular ordering of the emitted gluon in such a way that the emitted gluon lies within the opening angles of the  $q\text{--}\bar{q}$  pair,  $\theta_{q\bar{q}}$ . In the presence of a medium, as shown in Ref. [92, 93], the quark and the antiquark are subject to multiple scatterings along their trajectories that change their momenta, their distributions, and their propagating phases. These changes of the quark and antiquark sources of the gluon due to the medium will diminish the strength of the transverse coherent interference of the emitted gluon that occurs in the absence of the medium, leading to a gradual decoherence of the gluon emission as a function of increasing medium density [92, 93]. Recent experimental findings on reconstructed jets in nuclear collisions at the LHC [103, 104] suggest that such medium-induced partial decoherence may be an important effect.

Conventional model analysis of collision processes [77–81, 91–94] assumes the ladder-type diagrams such as Fig. 1(a) and Fig. 2(a), while the cross Feynman diagrams such as Fig. 1(b) and Figs. 2(b)–2(f) have been ignored. As the derivations in Section III demonstrate, the contributions from different cross diagrams destructively interfere with the ladder Feynman diagram and there is a

high degrees of cancellation. In general, the neglect of these destructive interference by including only the ladder Feynman diagram cannot be justified from a mathematical view point. Only in the special and restrictive case of quasi-elastic scattering with the fast particle assumed to be nearly on the mass shell and with the additional assumption of  $q_{i0} = 0$  is it justified to include only the ladder diagrams, at the expenses of precluding the exploration into other regions of scatterer recoils.

Many models have been proposed to explain the ridge phenomenon [31–38, 40–74]. They include the collision of jets with medium partons [31–38, 60, 61], flows and hydrodynamics with initial state fluctuations [40, 41, 48, 49, 57, 59, 66], color-glass condensate [47–49, 53, 58], modeling pQCD [62–65], parton cascade [67], gluon bremsstrahlung in string formation [68], strong-coupling AdS/CFT [70], quantum entanglement [72], and BFKL evolution and beyond [74]. There are however two difficulties associated with these phenomenological models. Almost all models deal with fragmented parts of the data and all models contain implicit and explicit assumptions.

In the presence of a large number of models and the above difficulties, progress can proceed in three fronts. First, the models need to cover an extensive set of experimental differential data over large phase spaces, centralities, and energies, from many different collaborations. Secondly, the assumptions of the models need further theoretical and observational investigations from fundamental viewpoints. Finally, experimental tests need to be proposed to distinguish different models.

With regard to the first of these three tasks, the momentum kick model gives reasonable descriptions for an extensive set of differential data of the ridge yield, over an extended range of transverse momenta, azimuthal angles, pseudorapidity angles, centralities, and collision energies, from the STAR Collaboration [1–5], the PHENIX Collaboration [20–23], the PHOBOS Collaboration [25], and the CMS Collaboration [26]. In these momentum kick model analyses, a collective longitudinal momentum kick on the medium scatterers along the jet direction is a central ingredient leading to the successful descriptions of the large set of experimental data. Additional analyses will be continued to extend the momentum kick model to include the effects of collective flows and to cover a larger set of new data as they become available.

With regard to the second of the three tasks, the momentum kick model contains the basic assumption that the  $\Delta\eta$  ridge arises mainly from the initial rapidity distribution of partons prior to the jet collision. Such a basic assumption has been examined from the viewpoint of the Wigner function of produced particles in a fundamental quantum theory of particle production [36]. Another basic assumption concerning the longitudinal nature of the momentum kick is now being examined in the present manuscript.

With regard to third of the three tasks, the present analysis for jets interacting with medium partons re-

veals that the longitudinal momentum kick is a quantum many-body effect that contains a threshold, requiring the multiple collisions of the jet with at least two partons. This may be in agreement with the onset of the ridge yield as a function of the centrality, observed by the CMS Collaboration for pp and PbPb collisions at LHC [100], and by the STAR Collaboration at RHIC [2, 14–18], as discussed in Section X. Furthermore, in the momentum kick model with longitudinal momentum kicks, the kicked medium partons from back-to-back jets possess a  $(p_{1T}, p_{2T})$  correlation for both the near side and the away side, as observed by the STAR Collaboration [18, 38].

It would be of interest to see how other proposed models fare with the three tasks at hand. It will also be of interest to see whether they contain the features of a rapid rise of the ridge yield as a function of the centrality, and the  $(p_{1T}, p_{2T})$  correlation for both the near side and the away side. The search for tests to distinguish different models will be an on-going research activity.

Whatever the theoretical descriptions, jets of order 10 GeV and below are known to be present in high-energy collisions [20–24, 75]. These jets collide with medium partons. They are not hydrodynamical flows, but they contribute to the azimuthal anisotropy and the azimuthal Fourier coefficients [105–107], as well as to two-particle

correlations. They must be taken into account or be subtracted from experimental data in theoretical models that do not include the jet effects explicitly.

In summary, Bose-Einstein interference in the passage of a jet in a dense medium is a quantum many-body effect that occurs quite generally in a coherent multiple collision process, with the threshold of more than two scatterers. The manifestation of the Bose-Einstein interference effect as collective recoils of the scatterers along the jet direction may have been experimentally observed in the  $\Delta\phi \sim 0$  correlation of hadrons associated with a high- $p_T$  trigger in high-energy AuAu collisions at RHIC, and pp and PbPb collisions at LHC. The experimental observation of ridge thresholds as a function of centrality may lend support for the occurrence of the Bose-Einstein interference thresholds in the passage of a jet in a dense medium.

### Acknowledgment

The author wishes to thank Profs. C. S. Lam, H. W. Crater, Jin-Hee Yoon, Vince Cianciolo, A. V. Koshelev, and Wei Li, for helpful discussions. This research was supported in part by the Division of Nuclear Physics, U.S. Department of Energy.

- 
- [1] J. Adams *et al.* for the STAR Collaboration, Phys. Rev. Lett. **95**, 152301 (2005).
  - [2] J. Adams *et al.* (STAR Collaboration), Phys. Rev. C **73**, 064907 (2006).
  - [3] J. Putschke (STAR Collaboration), J. Phys. **G34**, S679 (2007).
  - [4] J. Bielcikova (STAR Collaboration), J. Phys. **G34**, S929 (2007).
  - [5] F. Wang (STAR Collaboration), Invited talk at the XIth International Workshop on Correlation and Fluctuation in Multiparticle Production, Hangzhou, China, November 2007, [arXiv:0707.0815].
  - [6] J. Bielcikova (STAR Collaboration), Phys. **G34**:S929-930, 2007; J. Bielcikova for the STAR Collaboration, Talk presented at 23rd Winter Workshop on Nuclear Dynamics, Big Sky, Montana, USA, February 11-18, 2007, [arXiv:0707.3100]; J. Bielcikova for the STAR Collaboration, Talk presented at XLIII Rencontres de Moriond, QCD and High Energy Interactions, La Thuile, March 8-15, 2008, [arXiv:0806.2261].
  - [7] B. Abelev (STAR Collaboration), Talk presented at 23rd Winter Workshop on Nuclear Dynamics, Big Sky, Montana, USA, February 11-18, 2007, [arXiv:0705.3371].
  - [8] L. Molnar (STAR Collaboration), J. Phys. G **34**, S593 (2007).
  - [9] R. S. Longacre (STAR Collaboration), Int. J. Mod. Phys. **E16**, 2149 (2007).
  - [10] C. Nattrass (STAR Collaboration), J. Phys. G **35**, 104110 (2008).
  - [11] A. Feng, (STAR Collaboration), J. Phys. G **35**, 104082 (2008).
  - [12] P. K. Netrakanti (STAR Collaboration) J. Phys. G **35**, 104010 (2008).
  - [13] O. Barannikova (STAR Collaboration), J. Phys. G **35**, 104086 (2008).
  - [14] M. Daugherty, (STAR Collaboration), J. Phys. G **35**, 104090 (2008).
  - [15] D. Ray, in Talk presented at Tamura Symposium on Heavy Ion Physics, the University of Texas at Austin, November 2002, 2008, <http://www.ph.utexas.edu/~molly/tamura/>.
  - [16] D. Kettler, (STAR Collaboration), Euro. Phys. Jour. C, **62**, 175 (2009).
  - [17] G. Agakishiev *et al.*, (STAR Collaboration), arXiv:1109.4380 (2011).
  - [18] T. A. Trainor Phys. Rev. **C78**, 064908 (2008); T. A. Trainor and D. T. Kettler, Phys. Rev. D **74**, 034012 (2006); T. A. Trainor, Phys. Rev. C **80**, 044901 (2009); T. A. Trainor, J. Phys. G **37**, 085004 (2010).
  - [19] M. van Leeuwen, (STAR Collaboration), Eur. Phys. J. C **61**, 569 (2009).
  - [20] A. Adare, *et al.* (PHENIX Collaboration), Phys. Rev. C **78**, 014901 (2008).
  - [21] M. P. McCumber (PHENIX Collaboration), J. Phys. G **35**, 104081 (2008).
  - [22] Chin-Hao Chen (PHENIX Collaboration), “Studying the Medium Response by Two Particle Correlations”, Hard Probes 2008 Intern. Conf. on Hard Probes of High Energy Nuclear Collisions, A Toxa, Galicia, Spain, June 8-14, 2008.
  - [23] Jiangyong Jia, (PHENIX Collaboration), J. Phys. G **35**, 104082 (2008).



- 104033 (2008).
- [24] M.J. Tannenbaum, Eur. Phys. J. C **61**, 747 (2009).
- [25] E. Wenger (PHOBOS Collaboration), J. Phys. G **35**, 104080 (2008).
- [26] CMS Collaboration, JHEP **1009**, 091 (2010), [arXiv:1009.4122].
- [27] CMS Collaboration, arXiv:1105.2438 (2011).
- [28] CMS Collaboration, arXiv:1201.3158 (2012).
- [29] ATLAS Collaboration, arXiv:1203.3087 (2012).
- [30] ATLAS Collaboration, Phys. Lett. **B708**, 249 (2012).
- [31] C. Y. Wong, Phys. Rev. C **76**, 054908 (2007).
- [32] C. Y. Wong, Chin. Phys. Lett. **25**, 3936 (2008).
- [33] C. Y. Wong, J. Phys. G **35**, 104085 (2008).
- [34] C. Y. Wong, Phys. Rev. C **78**, 064905 (2008).
- [35] C. Y. Wong, Phys. Rev. C **80**, 034908 (2009).
- [36] C. Y. Wong, Phys. Rev. C **80**, 054917 (2009).
- [37] C. Y. Wong, Nonlin. Phenom. Complex Syst. **12**, 315 (2009), [arXiv:0911.3583].
- [38] C. Y. Wong, Phys. Rev. C **84**, 024901 (2011).
- [39] C. Y. Wong, Invited talk presented at the 35th Symposium on Nuclear Physics, Cocoyoc, Mexico, January 3, 2012, to be published in IOP Conference Series, [arXiv:1203.4441 (2012)].
- [40] E. Shuryak, Phys. Rev. C **76**, 047901 (2007).
- [41] S. A. Voloshin, Nucl. Phys. A **749**, 287 (2005).
- [42] C. B. Chiu and R. C. Hwa Phys. Rev. C **79**, 034901 (2009).
- [43] R. C. Hwa and C. B. Yang, Phys. Rev. C **67**, 034902 (2003); R. C. Hwa and Z. G. Tan, Phys. Rev. C **72**, 057902 (2005); R. C. Hwa and C. B. Yang, [nucl-th/0602024].
- [44] C. B. Chiu and R. C. Hwa Phys. Rev. C **72**, 034903 (2005).
- [45] R. C. Hwa, Phys. Lett. **B666**, 228 (2008).
- [46] V. S. Pantuev, [arXiv:0710.1882].
- [47] A. Dumitru, F. Gelis, L. McLerran, and R. Venugopalan, Nucl. Phys. A **810**, 91 (2008).
- [48] S. Gavin, and G. Moschelli, J. Phys. G **35**, 104084 (2008).
- [49] S. Gavin, L. McLerran, and G. Moschelli, Phys. Rev. C **79**, 051902 (2009).
- [50] N. Armesto, C. A. Salgado, and U. A. Wiedemann, Phys. Rev. Lett. **93**, 242301 (2004).
- [51] P. Romatschke, Phys. Rev. C **75**, 014901 (2007).
- [52] A. Majumder, B. Muller, and S. A. Bass, Phys. Rev. Lett. **99**, 042301 (2007).
- [53] A. Dumitru, Y. Nara, B. Schenke, and M. Strickland, Phys. Rev. C **78**, 024909 (2008); B. Schenke, A. Dumitru, Y. Nara, and M. Strickland, J. Phys. G **35**, 104109 (2008).
- [54] R. Mizukawa, T. Hirano, M. Isse, Y. Nara, and A. Ohnishi, J. Phys. G **35**, 104083 (2008).
- [55] Jianyong Jia and R. Lacey, Phys. Rev. C **79**, 011901 (2009).
- [56] Jianyong Jia, Eur. Phys. J. C **61**, 255 (2009).
- [57] Y. Hama, R. P. G. Andrade, F. Grassi, W.-L. Qian, Talk presented at ISMD2010, 21-25 September, 2010, University of Antwerp (Belgium), [arXiv:1012.1342]; R.P.G.Andrade, F.Gardim, F.Grassi, Y.Hama, W.L.Qian [arXiv:1107.0216].
- [58] A. Dumitru, K. Dusling, F. Gelis, J. Jalilian-Marian, T. Lappi, and R. Venugopalan, Phys. Lett. **B697**, 21 (2011), [arXiv:1009.5295].
- [59] K. Werner, Iu. Karpenko, K. Mikhailov, and T. Pierog [arXiv:1104.3269]; Fu-Ming Liu, K. Werner, [arXiv:1106.5909].
- [60] R. C. Hwa, C. B. Yang, Phys. Rev. C **83**, 024911 (2011), [arXiv:1011.0965].
- [61] C. B. Chiu and R. C. Hwa, [arXiv:1012.3486].
- [62] T. A. Trainor, arXiv:1008.4757; T. A. Trainor, arXiv:1011.6351; T. A. Trainor, arXiv:1012.2373.
- [63] T. A. Trainor and D. T. Kettler, Phys. Rev. C **83**, 034903 (2011).
- [64] T. A. Trainor and D. T. Kettler, arXiv:1010.3048.
- [65] T. A. Trainor and R. L. Ray, arXiv:1105.5428; R. L. Ray, arXiv:1106.5023.
- [66] B. Schenke, [arXiv:1106.6012]; B. Schenke, S. Jeon, C. Gale, [arXiv:1109.6289].
- [67] H. Petersen, C. Greiner, V. Bhattacharya, S. A. Bass, [arXiv:1105.0340].
- [68] B. A. Arbuzov, E. E. Boos, and V. I. Savrin, [arXiv:1104.1283].
- [69] M. Yu. Azarkin, I. M. Dremin, and A. V. Leonidov, [arXiv:1102.3258].
- [70] H. R. Grigoryan, and Y. V. Kovchegov, [arXiv:1012.5431].
- [71] I. Bautista, J. Dias de Deus, and C. Pajares, [arXiv:1011.1870].
- [72] I. O. Cherednikov and N. G. Stefanis, [arXiv:1010.4463].
- [73] I. M. Dremin, and V. T. Kim, [arXiv:1010.0918].
- [74] E. Levin, A. H. Rezaeian, [arXiv:1105.3275].
- [75] X. N. Wang and M. Gyulassy, Phys. Rev. D **44**, 3501 (1991); X. N. Wang and M. Gyulassy, Phys. Rev. Lett. **68**, 1480 (1992).
- [76] J. D. Bjorken, Fermilab-Pub-82-059-THY (1982).
- [77] M. Gyulassy and X. N. Wang, Nucl. Phys. **B420**, 583 (1994).
- [78] R. Baier, Yu. L. Dokshitzer, A. H. S. Peigne, and D. Schiff, Nucl. Phys. **B478**, 577 (1996).
- [79] U. A. Wiedemann, Nucl. Phys. **B582**, 409 (2000).
- [80] M. Gyulassy, P. Levai, and I. Vitev, Nucl. Phys. **B594**, 371 (2001).
- [81] M. Djordjevic and M. Gyulassy, Nucl. Phys. **A733**, 265 (2004).
- [82] S. S. Adler *et al.* (PHENIX Collaboration), Phys. Rev. **C69**, 034910 (2004); J. Adam *et al.* (STAR Collaboration), Phys. Rev. Lett. **91**, 172302 (2003); B. B. Back *et al.* (PHOBOS Collaboration), Phys. Lett. **B578**, 297 (2004); I. Arsene *et al.* (BRAHMS Collaboration), Phys. Rev. Lett. **91**, 072305 (2003); B. I. Abelev *et al.* (STAR Collaboration), Phys. Rev. Lett. **98**, 192301 (2007); S. S. Adare *et al.* (PHENIX Collaboration), Phys. Rev. Lett. **97**, 252002 (2006).
- [83] H. Cheng and T. T. Wu, Phys. Rev. **186**, 1611 (1969).
- [84] H. Cheng and T. T. Wu, *Expanding Protons: Scattering at High Energies*, M. I. T. Press, 1987.
- [85] Y. J. Feng, O. Hamidi-Ravari, and C. S. Lam, Phys. Rev. D **54**, 3114 (1996).
- [86] Y. J. Feng, O. Hamidi-Ravari, and C. S. Lam, Phys. Rev. D **55**, 4016 (1997).
- [87] C. S. Lam, Lectures given at the First Asia Pacific Workshop on Strong Interactions, Taipei. August 1st to 27th, 1996, hep-ph/9704240.
- [88] C. S. Lam and K.F. Liu, Nucl. Phys. **B483**, 514 (1997).
- [89] C. S. Lam and K.F. Liu, Phys. Rev. Lett. **79**, 597 (1997).
- [90] C. S. Lam, Chin. Jour. Phys. **35**, 758 (1997), hep-ph/9805210.
- [91] G. Ovanessian and I. Vitev, JHEP **1106** (2011) 080.

- [92] Y. Mehtar-Tani, C.A. Salgado, and K. Tywoniuk, J.Phys. **G38**, 124063 (2011).
- [93] N. Armesto, Hao Ma, Y. Mehtar-Tani, C. A. Salgado, K. Tywoniuk, JHEP **1201**, 109 (2012),
- [94] R. J. Glauber, in *Lectures in Theoretical Physics*, edited by W. E. Brittin and L. G. Dunham (Interscience, N.Y., 1959), Vol. 1, p. 315.
- [95] In this manuscript, we use the Feynman rule in Ref. [84] which includes explicitly an overall multiplicative phase factor of  $(-i)$ . Such a overall phase  $(-i)$  is not explicitly stated but implicitly implied in Appendix A-4 of Ref. [96].
- [96] C. Itzykson and J.B. Zuber, *Quantum Field Theory*, McGraw Hill, (1980).
- [97] V. B. Berestetskii, E. M. Lifshitz, and L. P. Pitaevskii, *Quantum Electrodynamics*, Pergamon Press, 1982.
- [98] C. Y. Lo and H. Cheng, Phys. Rev. D**13**, 1131 (1976); P. S. Yeung, Phys. Rev. D **13**, 23062317 (1976).
- [99] H. Cheng, J. A. Dickinson, and K. Olausen, Phys. Rev. D **23**, 534 (1981).
- [100] CMS Collaboration, in CMS Physics Analysis Summary HIN-11-006, available on the CERN CDS Information Server at <http://cdsweb.cern.ch/record/1353583/files/HIN-11-006-pas.pdf>.
- [101] M. E. Peskin and D. V. Schroeder *An Introduction To Quantum Field Theory*, Addison-Wesley Publishing Company, (1995).
- [102] R. J. Glauber, in *High-Energy Physics and Nuclear Structure*, edited by S. Devons, Press Press, N.Y. , 1970.
- [103] G. Aad *et al.* (Atlas Collaboration), Phys. Rev. Lett. **105**, 252303 (2010), arXiv:1011.6182.
- [104] S. Chatrchyan *et al.* (CMS Collaboration), Phys. Rev. **C84** , 024906 (2011), arXiv:1102.1957.
- [105] C. Y. Wong, Phys. Lett. B **88**, 39 (1979).
- [106] J. Y. Ollitrault, Phys. Rev. D **46**, 229 (1992).
- [107] S. Voloshin, Y. Zhang, Z. Phys. Rev. C **70**, 665 (1996).